DAFTAR PUSTAKA

Abid, Z., Hakiki, A., Boukoussa, B., Launay, F., Hamaizi, H.,Bengueddach, A., & Hamacha, R. 2019. Preparation of highly hydrophilic PVA/SBA-15 composite materials and their adsorption behaviour toward cationic dye: effect of PVA content. *Journal of materials science*, *54*(10), 7679-7691.

Admi, A., Ramadhani, F., & Syukri, S. 2020. Sintesis dan Karakterisasi Enkapsulat Katalis Nikel (II) pada Silika Mesopori Modifikasi. *Jurnal Riset Kimia*, *11*(2), 89-96.

Ahmed, S., Ramli, A., & Yusup, S. 2016. CO_2 adsorption study on primary, secondary and tertiary amine functionalized Si-MCM 41. *International Journal of Greenhouse Gas Control*, *51*, 230-238.

Ahmed, S., Ramli, A., & Yusup, S. 2017. Development of polyethylenimine-functionalized mesoporous Si-MCM-41 for CO_2 adsorption. *Fuel Processing Technology*, *167*, 622-630.

Al-Degs, Y. S., El-Barghouthina, M. I., Issa, A. A., Khraishebb, M. A.,Walker,G.M. 2006. Sorption of Zn(II), Pb(II), and Co(II) using natural adsorbents: Equilibrium and Kinetic Studies. *Water Research*, *40*, 2645–2658.

Almeida, J.M.F., Oliveira, É.S., Silva, I.N., De Souza, S.P.M.C., Fernandes, N.S., 2017. Adsorption of erichrome black T from aqueous solution onto expanded perlite modified with orthophenanthroline. *Rev. Virtual Quim*. *9*(2), 502–513.

Anirudhan, T.S., Radhakrishnan, P.G. 2008. Thermodynamics and kinetic adsoption of Cu(II) from aquoeous solution onto a new cation exchanger derived from tamarind fruit shell. *Journal Chemical Thermodynamics*, *40*, 702–709.

Anita, S. H., Sari, F. P., & Yanto, D. H. Y. 2019. Decolorization of synthetic dyes by ligninolytic enzymes from trametes hirsuta D7. *Makara Journal of Science*, *23*(1), 44–50.

Arzani, K., Behdad, G. A., & Amirhossein, H. A. K. 2012. Equilibrium and kinetic adsorption study of the removal of Orange-G dye using carbon mesoporous material. *Journal of Inorganic Materials*, *27*(6), 660–666.

Asria, M., & Alhamid, F. 2020. Analisis Kandungan Logam Berat Cu dan Zn dalam Air Limbah Industri. *REACTOR: Journal of Research on Chemistry and Engineering*, *1*(2), 29-31.

Beck, J. S., Vartuli, J. C., Roth, W. J., Leonowicz, M. E., Kresge, C. T., Schmitt, K. D., & Schlenker, J. 1992. A new family of mesoporous molecular sieves prepared with liquid crystal templates. *Journal of the American Chemical Society*, *114*(27), 10834-10843.

Benkhaya, S., El Harfi, S., & El Harfi, A. 2017. Classifications, properties and applications of textile dyes: A review. *Applied Journal of Environmental Engineering Science,* 3(3), 311-320.

Benkhaya, S., M' rabet, S., & El Harfi, A. 2020. A review on classifications, recent synthesis and applications of textile dyes. *Inorganic Chemistry Communications*, *115*, 1–35.

Bhattacharyya, K.G., Gupta, S.S. 2008. Influence of Acid activaton on Adsoption of Ni(II) and Cu(II) on Kaolinite and Montmorillonite: Kinetic and Thermo-dynamic Study. *Chemical Engineering Journal*, *136*, 1–13.

Bhernama, B. G., Safni, S., & Syukri, S. 2015. Degradasi Zat Warna Metanil Yellow dengan Penyinaran Matahari dan Penambahan Katalis TiO_2-SnO_2. *Lantanida Journal*, *3*(2), 116-126.

Boukoussa, B., Hamacha, R., Morsli, A., & Bengueddach, A. 2017. Adsorption of yellow dye on calcined or uncalcined Al-MCM-41 mesoporous materials. *Arabian Journal of Chemistry*, *10*, S2160-S2169.

Boukoussa, B., Hakiki, A., Moulai, S., Chikh, K., Kherroub, D. E., Bouhadjar, L., & Hamacha, R. 2018. Adsorption behaviors of cationic and anionic dyes from aqueous solution on nanocomposite polypyrrole/SBA-15. *Journal of materials science*, *53*(10), 7372-7386.

Burkett, S. L., Sims, S. D., & Mann, S. 1996. Synthesis of hybrid inorganic-organic mesoporous silica by co-condensation of siloxane and organosiloxane precursors. *Chemical Communications, 11*, 1367-1368.

Brown, M. A., & De Vito, S. C. 1993. Predicting azo dye toxicity. *Critical reviews in environmental science and technology*, *23*(3), 249-324.

Cakiryilmaz, N., Arbag, H., Oktar, N., Dogu, G., & Dogu, T. 2019. Catalytic performance of Ni and Cu impregnated MCM-41 and Zr-MCM-41 for hydrogen production through steam reforming of acetic acid. *Catalysis Today,* 323, 191-199.

Chen, J., N. Xia, T. Zhou, S. Tan and F. Jiang. 2009. Mesoporous carbon spheres: synthesis, characterization and supercapacitance*. International Journal of Electrochemical Science,* 4, 1063-1073.

Chen, B., Long, F., Chen, S., Cao, Y., & Pan, X. 2020. Magnetic chitosan biopolymer as a versatile adsorbent for simultaneous and synergistic removal of different sorts of dyestuffs from simulated wastewater. *Chemical Engineering Journal*, *385*, 123-130.

Costa, J. A., Garcia, A. C., Santos, D. O., Sarmento, V. H., Porto, A. L., Mesquita, M. E. D., & Romão, L. P. 2014. A new functionalized MCM-41 mesoporous material for use in environmental applications. *Journal of the Brazilian Chemical Society*, *25*(2), 197- 207.

Costa, J. A., Garcia, A. C., Santos, D. O., Sarmento, V. H., de Mesquita,M. E., & Romao, L. P. 2015. Applications of inorganic–organic mesoporous materials constructed by self-assembly processes for removal of benzo [k]

fluoranthene and benzo [b] fluoranthene. *Journal of Sol-Gel Science and Technology*, *75*(3), 495-507.

Costa, J. A. S., de Jesus, R. A., da Silva, C. M. P., & Romão, L. P. C. 2017.Efficient adsorption of a mixture of polycyclic aromatic hydrocarbons (PAHs) by Si–MCM–41 mesoporous molecular sieve. *Powder Technology*, *308*, 434-441.

Costa, J. A. S., de Jesus, R. A., Santos, D. O., Mano, J. F., Romao, L. P., & Paranhos, C. M. 2020. Recent progresses in the adsorption of organic, inorganic, and gas compounds by MCM-41-based mesoporous materials. *Microporous and Mesoporous Materials*, *291*, 109698.

Crini, G., Peindy, H.N., Gimbert, F., & Robert, C. 2007. Removal of C.I basic green 4 (malachite green) from aqueous solutions by adsorption using cyclo dextrin-based adsorbent: kinetic and equilibrium studies. *Separation and Purification Technology*, *53*, 97–110

Dehghani, S., Haghighi, M., & Vardast, N. 2019. Structural/texture evolution of CaO/MCM-41 nanocatalyst by doping various amounts of cerium for active and stable catalyst: biodiesel production from waste vegetable cooking oil. *International Journal of Energy Research*, 43(8), 3779-3793.

Dhal, J.P., Dash, T. & Hota, G. 2020. Iron oxide impregnated mesoporous MCM-41: synthesis, characterization and adsorption studies. *Journal of Porous Materials*, 27(1), 205–216.

Dinh Du, P., Hieu, N. T., To, T. C., Bach, L. G., Tinh, M. X., Xuan Mau, T., & Quang Khieu, D. 2019. Aminopropyl functionalised MCM-41: synthesis and application for adsorption of Pb (II) and Cd (II). *Advances in Materials Science and Engineering* (2019), 1-15.

Dubois, M., Gulik-Krzywicki, T., & Cabane, B. 1993. Growth of silica polymers in a lamellar mesophase. *Langmuir*, *9*(3), 673-680.

Fatima, B., Siddiqui, S.I., Ahmed, R., & Chaudry, S.A. 2019. Green synthesis of f-$CdWO_4$ for photocatalytic degradation and adsorptive removal of Bismarck Brown R dye from water. *Water Resources and Industry*, 22, 100-119.

Fauzia, S., Furqani, F., Zein, R. & Munaf, E. 2015. Adsorption and reaction kinetics of tatrazine by using *Annona muricata* L seeds. *Journal of Chemical and Pharmaceutical Research, 7*(1), 573–582.

Fedeyko, J.M., D.G. Vlachos & R.F. Lobo. 2006. Understanding the differences between microporous and mesoporous synthesis through the phase behavior of silica. *Microporous Mesoporous Material., 90*, 102-111.

Fitriah, H., Mahatmanti, F. W., & Wahyuni, S. 2012. Pengaruh konsentrasi pada pembuatan membran kitosan terhadap selektivitas ion Zn (II) dan Fe (II). *Indonesian Journal of Chemical Science*, *1*(2), 104-109.

Garcia, F. A., Braga, V. S., Silva, J. C., Dias, J. A., Dias, S. C., & Davo, J. L. 2007. Acidic characterization of copper oxide and niobium pentoxide supported on silica–alumina. *Catalysis letters*, *119*(1), 101-107.

Girolami, M. W., & Rousseau, R. W. 1985. Effects of bismarck brown R on the growth rates of large and small potassium alum crystals. *Journal of Crystal Growth*, *71*(1), 220-224.

Gleizes, A.N., Fernandes, A., & Dexpert-Ghys, J. 2004. Grafting 4f and 3d metal complexes into mesoporous MCM-41 silica by wet impregnation and by chemical vapour infiltration. *Journal of Alloys and Compounds,* 374(2), 303-306.

Guo, Y., Liu, D., Zhao, Y., Gong, B., Guo Y., & Huang, W. 2017. Synthesis of chitosan-functionalizes MCM-41-A and its performances in Pb(II) removal from synthetic water. *Journal of Taiwan Institute of Chemical Engineers*, 71, 537-545.

Guo, Y. H., Pan, G. X., Xu, M. H., Wu, T., & Wang, Y. Y. 2019. Synthesis and Adsorption Desulfurization Performance of Modified Mesoporous Silica Materials M-MCM-41 (M= Fe, Co, Zn). *Clays and Clay Minerals*, *67*(4), 325-333.

Gupta, S. S., Bhattacharyya, K. G. 2005. Interaction of metal ions with clays: A case study with Pb(II). *Applied Clay Science*, *30*, 199–208.

Gupta, S. S. & Babu, B. V. 2009. Removal of toxic metal Cr(VI) from aqueous solution using sawdust as adsorbent: Equilibrium, kinetics and regeneration studies. *Chemical Engineering Journal*, *150*, 352– 365.

Hachemaoui, M., Boukoussa, B., Mokhtar, A., Mekki, A., Beldjilali, M., Benaissa, M., & Hamacha, R. 2020. Dyes adsorption, antifungal and antibacterial properties of metal loaded mesoporous silica: Effect of metal and calcination treatment. *Materials Chemistry and Physics*, *256*, 123-704.

Han, B., Zhang, F., Feng, Z., Liu, S., Deng, S., Wang, Y., & Wang, Y. 2014. A designed Mn_2O_3/MCM-41 nanoporous composite for methylene blue and rhodamine B removal with high efficiency. *Ceramics International*, 40(6), 8093-8101.

Hasanah N., Sutarno. & Kunarti E.S. 2018 Kajian Karakteristik MCM-41 yang dimodifikasi dengan logam Zn secara direct synthesis. *Jurnal Kimia dan Pendidikan Kimia, 3*(3), 183-192.

Hermawati, E. S., Suhartana, S., & Taslimah, T. 2016. Sintesis dan karakterisasi senyawa kompleks Zn (II)-8-hidroksikuinolin. *Jurnal Kimia Sains dan Aplikasi*, *19*(3), 94-98.

Huang, Kai, Zhili Wang, & Dongfang Wu. 2018. Synthesis of well-ordered MCM-41 containing highly-dispersed NiO nanoparticles and efficient catalytic epoxidation of styrene. *Journal of Chemical Sciences*. 130(6), 1-12.

Hussein, F.H., & Halbus, A.F. 2012. Rapid decolorization of cobalamin. *International Journal of Photoenergy, 2012,* 75-83.

Inbaraj, B. S., & Chen, B. H. 2011. Dye adsorption characteristics of magnetite nanoparticles coated with a biopolymer poly (γ-glutamic acid). *Bioresource technology*, *102*(19), 8868-8876.

Indihani, R.R., Nugroho, W.A., & Lutfi, M. 2019. Pengaruh konsentrasi aktivator arang aktif dan waktu kontak limbah terhadap kandungan TDS dan zat warna limbah cair batik. *Jurnal Keteknikan Pertanian Tropis dan Biosistem, 5*(3), 281-288.

Julinawati, J., Marlina, M., Nasution, R., & Sheilatina, S. 2015. Applying SEM-EDX techniques to identifying the types of mineral of jades (giok) Takengon, Aceh. *Jurnal Natural Unsyiah*, *15*(2), 116128.

Kamil, A. M., Abdalrazak, F. H., Halbus, A. F., & Hussein, F. H. 2014. Adsorption of bismarck brown R dye onto multiwall carbon nanotubes. *Journal of Environmental Analytical Chemistry*, *1*(104), 2-5.

Karyasa, I. W. 2013. Studi X-Ray Fluoresence dan X-Ray diffraction terhadap Bidang Belah Batu Pipih Asal Tejakula. *Jurnal Sains dan Teknologi, 2*(2), 1-9.

Kustomo, K., & Santosa, S. J. 2019. Adsorption and Kinetic Studies of Cationic (Methylene Blue) and Anionic (Methyl Orange) Dyes onto Magnetite Coated with Humic Acid. *Jurnal Jejaring Matematika dan Sains*, *1*(2), 64-69.

Kresge, C. T., Vartuli, J. C., Roth, W. J., & Leonowicz, M. E. 2004. The discovery of ExxonMobil's M41S family of mesoporous molecular sieves. *Studies in Surface Science and Catalysis*, *148*, 53-72.

Laksaci, H., Khelifi, A., Belhamdi, B., & Trari, M. 2018. The use of prepared activated carbon as adsorbent for the removal of orange G from aqueous solution. *Microchemical Journal,* 145, 908-913.

Lynch, V. & Laura, M. 2017. Introduction to Micro-residues Analysis: Systematic use of Scanning Electron Microscope and Energy Dispersive X-rays Spectroscopy (SEM-EDX) on Patagonian Raw Materials*. Journal of Archaeological Science: Reports*, *16*(3), 299-308.

Mane, V. S., Mall, I. D. & Srivasta, V. C. 2007. Kinetic equilibrium isotherm studies for adsorptive removal of brilliant green dye from aqueous solution by rice husk ash. *Journal of Enviromental Management*, 84, 390–400.

Mathew, A., Parambadath, S., Barnabas, M. J., Song, H. J., Kim, J. S., Park, S. S., & Ha, C. S. 2016. Rhodamine 6G assisted adsorption of metanil yellow over succinamic acid functionalized MCM-41. *Dyes and Pigments*, *131*, 177-185.

McCusker, Liebau, L.B., F. & G. Engelhardt, 2003. Nomenclature of structural and compositional characteristics of ordered microporous

and mesoporous materials with inorganic hosts: (IUPAC recommendations 2001). *Microporous Mesoporous Material*., *58,* 3-13.

Meléndez-Ortiz, H. I., García-Cerda, L. A., Olivares-Maldonado, Y., Castruita, G.,Mercado-Silva, J. A., & Perera-Mercado, Y. A. 2012. Preparation of spherical MCM-41 molecular sieve at room temperature: Influence of the synthesis conditions in the structural properties. *Ceramics International*, *38*(8), 6353-6358.

Mizhir, A., Abdulwahid, A., & Al-Lami, H. 2020. Chemical functionalization graphene oxide for the adsorption behavior of bismarck brown dye from aqueous solutions. *Egyptian Journal of Chemistry*, *63*(5), 1679-1696.

Mobarak, M., Mohamed, E. A., Selim, A. Q., Eissa, M. F., & Seliem, M. K. 2019. Experimental results and theoretical statistical modelling of malachite green adsorption onto MCM–41 silica/rice husk composite modified by beta radiation. *Journal of Molecular Liquids*, *273*, 68-82.

Mokhonoana, M.P., & Coville, N.J. 2010. Synthesis of [Si]-MCM-41 from TEOS and water glass: the water glass-enhanced condensation of TEOS under alkaline conditions. *Journal of Sol-Gel Science and Technology, 54*(1), 83-92.

Munasir, M., Triwikantoro, T., Zainuri, M., & Darminto, D. 2012. Uji XRD dan XRF pada bahan meneral (batuan dan pasir) sebagai sumber material cerdas ($CaCO_3$ dan SiO_2). *Jurnal Penelitian Fisika dan Aplikasinya (JPFA)*, *2*(1), 20-29.

Naiya, T. K., Clowdhury, P., Bhattacharya, A. K., Das, S. K. 2009. Sawdust and neem bark as low cost natural biosorbent for adsorptive removal of Zn(II) and Cd(II) ions from aqueous solutions, *Chemical Engineering Journal*, *148*, 79-86.

Nagappan, S., Jeon, Y., Park, S.S., & Ha, C.S. 2019. Hexadecyl-trimethylammonium bromide surfactant-supported silica material for the effective adsorption of metanil yellow dye. *ACS Omega,* 4(5), 8548-8558.

Nandiyanto, A., Kim, S.G. Iskandar, F. & Okuyama, K. 2009. Synthesis of spherical mesoporous silica nanoparticles with nanometer-size controllable pores and outer diameters. *Microporous Mesoporous Material*., 120: 447-453.

On, D. T., Desplantier-Giscard, D., Danumah, C., & Kaliaguine, S. 2003. Perspectives in catalytic applications of mesostructured materials. *Applied Catalysis A: General*, *253*(2), 543-553.

Oshima, S., Perera, J.M., Northcott, K.A., Kokusen, H., Stevens, G.W., Komatsu, Y. 2006. Adsorption behaviour of cadmium(II) and lead(II) on mesoporous silicate MCM-41. *Separation Science and Technology,* 41(8), 1635-1643.

Piaskowski, K., Swiderska-dabrowska, R., & Zarzycki, P.K. 2018. Dye removal from water and wastewater using various physical, chemical and biological processes. *Journal of AOAC International,* 101(5), 1371-1384.

Purnawira, B., Purwaningsih, H., Ervianto, Y., Pratiwi, V.M., Susanti, D., Rochiem, R., & Purniawan, A. 2019.Synthesis and characterization of mesoporous silica nanoparticles (MSNp) MCM-41 from natural waste rice husk. *IOP Conferences Series: Materials Science and Engineering,* 541(1), 12-18.

Putra, S. E., Khairuddin, K., Puspitasari, D. J., & Sosidi, H. 2019. Pemanfaatan Karbon Aktif Ampas Tahu Teraktivasi NaCl Sebagai Penyerap Zat Warna Congo Red. *Kovalen: Jurnal Riset Kimia*, *5*(1), 109-115.

Qin, Q., Ma, J., & Liu, K. 2009. Adsorption of anionic dyes on ammonium-functionalized MCM-41. *Journal of Hazardous Materials*, *162*(1), 133-139.

Rahman, M. M., Aznan, M. A. B. M., Yusof, A. M., Ansary, R. H., Siddiqi, M. J., & Yusan, S. 2017. Synthesis and Characterization of Functionalized Se-MCM-41 a New Drug Carrier Mesopore Composite. *Oriental Journal of Chemistry*, *33*(2), 611.

Rao, Y. & Antonelli, D.M. 2009. Mesoporous transition metal oxides: characterization and applications in heterogeneous catalysis. *Journal of Materials Chemistry,* 19, 1937-1944.

Rápó, E., & Tonk, S. 2021. Factors affecting synthetic dye adsorption; desorption studies: a review of results from the last five years (2017–2021). *Molecules*, *26*(17), 5419-5450.

Raya, I., Widjaja, G., Mahmood, Z. H., Kadhim, A. J., Vladimirovich, K. O., Mustafa, Y. F., & Kafi-Ahmadi, L. 2022. Kinetic, isotherm, and thermodynamic studies on Cr(VI) adsorption using cellulose acetate/graphene oxide composite nanofibers. *Applied Physics A*, *128*(2), 1-9.

Ridhawati, A. W. Wahab, N. L. Nafie, I. Raya. 2018. Pengaruh Metode Sintesis Silika Mesopori SBA-15 terhadap Analisis Differential Scanning Calorimetry dan Pengukuran Low Angles X-Ray Diffraction*. Journal INTEK*. *5*(1), 39-43.

Rosales, E., Meijide, J., Tavares, T., Pazos, M., & Sanromán, M.A. 2016. Grapefruit peelings as a promising biosorbent for the removal of leather dyes and hexavalent chromium. *Process Safety and Environmental Protection, 101*, 61–71.

Ryoo, R., Ko, C. H., & Howe, R. F.1997. Imaging the distribution of framework aluminum in mesoporous molecular sieve MCM-41. *Chemistry of materials*, *9*(7), 1607-1613.

Saba, B., Christy, A. D., & Jabeen, M. 2016. Kinetic and enzymatic decolorization of industrial dyes utilizing plant-based biosorbents: a review. *Environmental Engineering Science*, *33*(9), 601-614.

Safni, S., Sari, F., Maizatisna, M., & Zulfarman, Z. 2009. Degradasi Zat warna Methanil Yellow Secara Sonolisis dan Fotolisis dengan Penambahan TiO_2 Anatase. *Jurnal Sains Materi Indonesia*, *11*(1), 47-51.

Sahoo, D.P., Rath, D., Nanda, B., & Parida, K.M. 2015. Transition metal/metal oxide modified MCM-41 for pollutant degradation and hydrogen energy production: a review. *RSC advances*. 5(102), 83707- 83724.

Santos, D.O., Santos, M.D.L.N., Costa, J.A.S., de Jesus, R.A., Navickiene, S., Sussuchi, E.M., & de Mesquita, M.E. 2013. Investigating the potential of functionalized MCM-41 on adsorption of remazol red dye. *Environmental Science and Pollution Research, 20*(7), 5028-5035.

Sari, R. A., Firdaus, M. L., & Elvia, R. 2017. Penentuan Kesetimbangan, Termodinamika dan Kinetika Adsorpsi Arang Aktif Tempurung Kelapa Sawit Pada Zat Warna Reactive Red dan Direct Blue. *Jurnal Ilmu Pendidikan Kimia*, *1*(1), 10-14.

Sayari, A. 1996. Periodic mesoporous materials: synthesis, characterization and potential applications. *Studies in Surface Science and Catalysis, 102*, 1–46.

Shu, Y., Shao, Y., Wei, X., Wang, X., Sun, Q., Zhang, Q., & Li, L. 2015. Synthesis and characterization of Ni-MCM-41 for methyl blue adsorption. *Microporous and Mesoporous Materials*, *214*, 88-94.

Sleiman, M., Vildozo, D., Ferronato, C., & Chovelon, J.M. 2007. Photocatalytic degradation of azo dye metanil yellow: optimization and kinetic modelling using a chemometric approach. *Applied Catalysis B: Environmental,* 77(1), 1-11.

Soriano, J.J., Mathieu-Denoncourt, J., Norman, G., De Solla, S.R., & Langlois, V.S. 2014. Toxicity of the azo dyes acid red 97 and bismarck brown Y to western clawed frog (silurana tropicalis). *Environmental Science and Pollution Research,* 21(5), 3582-3591.

Taba, P. 2008. Adsorption of Water and Benzene Vapour in Mesoporous Materials. *Makara Journal of Science*, *12*(2), 120-125.

Tariq, M. A., Faisal, M., & Muneer, M. 2005. Semiconductor-mediated photocatalysed degradation of two selected azo dye derivatives, amaranth and bismarck brown in aqueous suspension. *Journal of Hazardous Materials*, 127(1), 172-179.

Tengker, S., & Falah, I. 2017. Sintesis dan karakterisasi material mesopori MCM-41 menggunakan TMAOH dan garam anorganik K_2SO_4. *Fullerene Journal of Chemistry,* 2(2), 61-65.

Tong, Y., McNamara, P.J., & Mayer, B.K. 2019. Adsorption of organic micropollutants onto biochar: a review of relevant kinetics, mechanisms and equilibrium. *Environmental Science: Water Research & Technology, 5*(5), 821-838.

Vartuli, J. C., Schmitt, K. D., Kresge, C. T., Roth, W. J., Leonowicz, M. E., McCullen, S. B., & Sheppard, E. W. 1994. Development of a formation mechanism for M41S materials. *Studies in Surface Science and Catalysis*, *84*, 53-60.

Vartuli, J.C., W.J. Roth and T.F. Degnan, 2008. *Mesoporous materials (M41S): From discovery to application. Dekker Encyclopedia of Nanoscience and Nanotechnology*, Taylor and Francis: New York.

Xia, Y. and R. Mokaya, 2003. A study of the behavior of mesoporous silicas in OH/CTABr/H2O systems: phase dependent stabilisation, dissolution or semipseudomorphic transformation. *Journal of Materials Chemistry*, *13*, 3112-3121.

Xu, B., J. Long, H. Tian, Y. Zhu and X. Sun, 2009. Synthesis and characterization of mesoporous [gamma]-alumina templated by saccharide molecules. *Catalysis Today*, *147,* 46-50.

Yanagisawa, T., Shimizu, T., & Kuroda, K. 1990. The preparation of alkyltrimethylammonium-kanemite complexes and their conversion to microporous materials. *Chemical Society of Japan Journals, 63*(4), 988-992.

Zaidi, Z., Siddiqui, S. I., Fatima, B., & Chaudhry, S. A. 2019. Synthesis of ZnO nanospheres for water treatment through adsorption and photocatalytic degradation: Modelling and process optimization. *Materials Research Bulletin*, *120*, 11-584.

Zein, R., Astuti, A.W., Wahyuni, D., Furqani, F., Munaf, E., 2015. Removal of Methyl Red from Aqueous Solution by Neplhelium lappaceum. *Research Journal of Pharmaceutical, Biological and Chemical Sciences, 6(3)*, 86–97.

Zein, R., Ramadhani, P., Aziz, H., & Suhaili, R. 2019. Biosorben cangkang pensi (Corbicula moltkiana) sebagai penyerap zat warna metanil yellow ditinjau dari pH dan model kesetimbangan adsorpsi. *Jurnal Litbang Industri*, 9(1), 15-22.

Zhao, X. S., Lu, G. Q., & Millar, G. J. 1996. Advances in mesoporous molecular sieve MCM-41. *Industrial & Engineering Chemistry Research*, *35*(7), 2075-2090.

Zhou, C., Gao, Q., Luo, W., Zhou, Q., Wang, H., Yan, C., & Duan, P. 2015. Preparation, characterization and adsorption evaluation of spherical mesoporous Al-MCM-41 from coal fly ash. *Journal of the Taiwan Institute of Chemical Engineers*, *52*, 147-157.

Lampiran 1. Skema Sintesis Silika Mesopori MCM-41

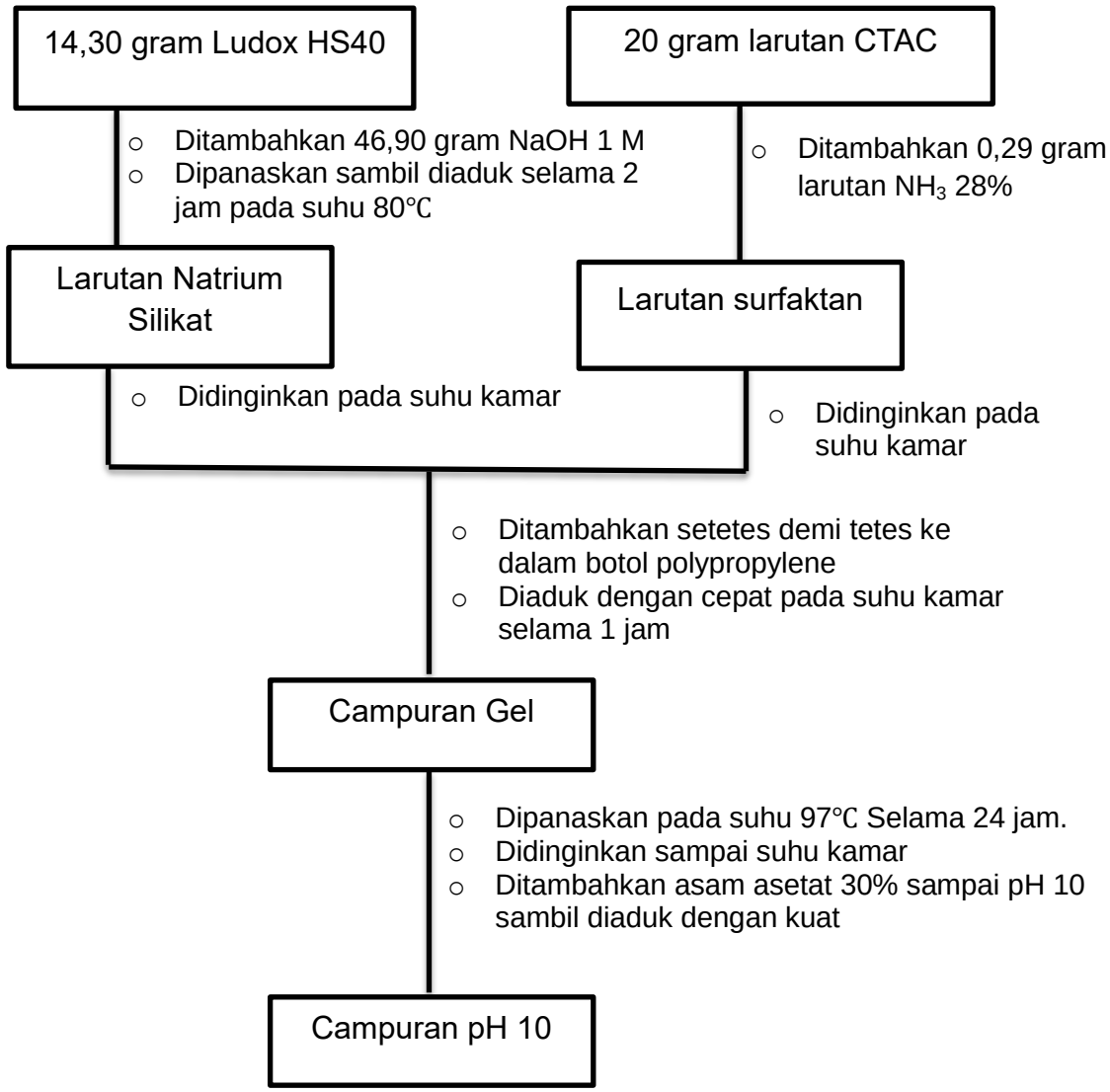

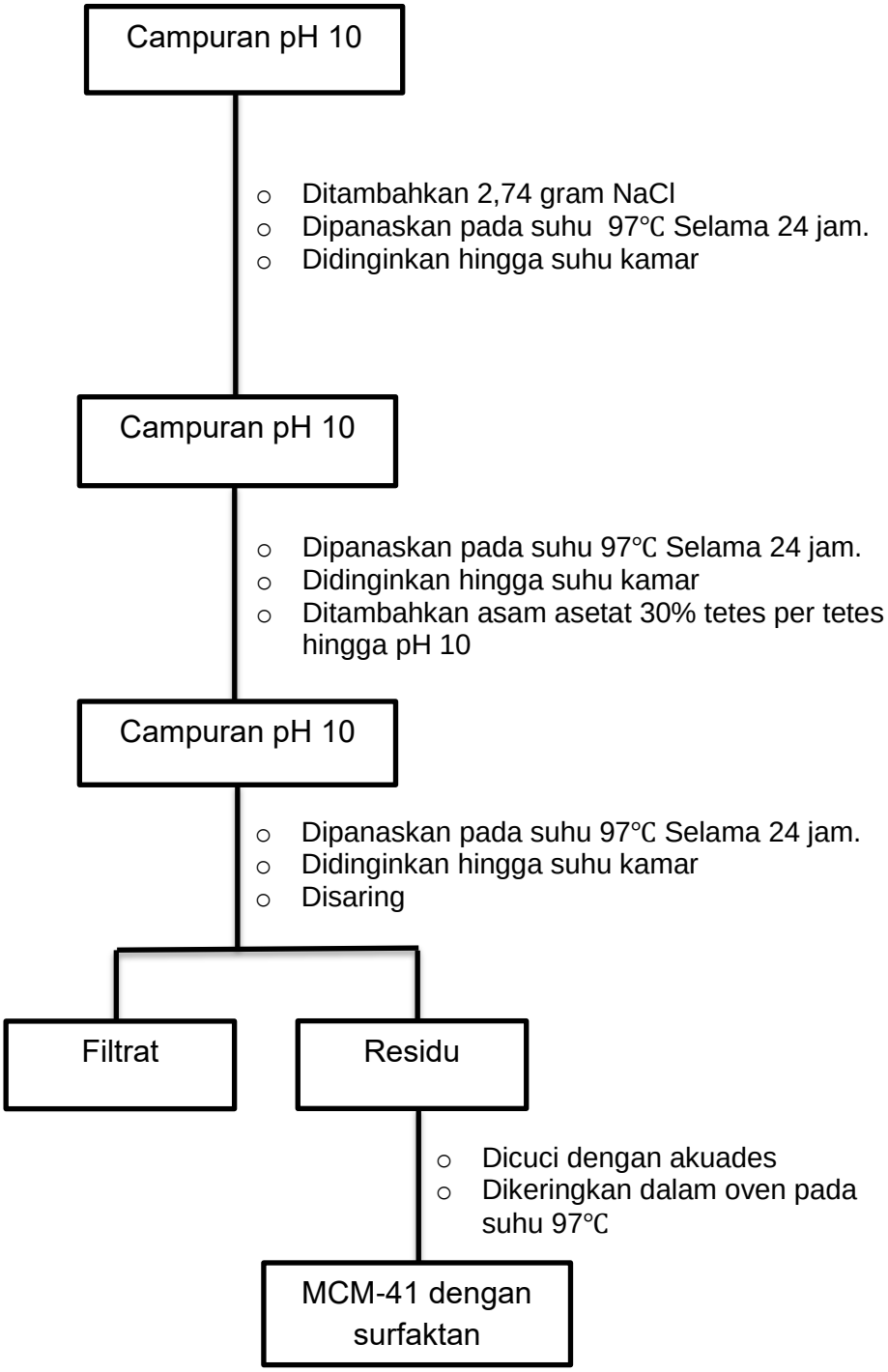
Campuran pH 10
Ditambahkan 2,74 gram NaCl
Dipanaskan pada suhu 97℃ Selama 24 jam.
Didinginkan hingga suhu kamar
Campuran pH 10
Dipanaskan pada suhu 97℃ Selama 24 jam.
Didinginkan hingga suhu kamar
Ditambahkan asam asetat 30% tetes per tetes hingga pH 10
Campuran pH 10
Dipanaskan pada suhu 97℃ Selama 24 jam.
Didinginkan hingga suhu kamar
Disaring
Filtrat
Residu
Dicuci dengan akuades
Dikeringkan dalam oven pada suhu 97℃
MCM-41 dengan surfaktan

Lampiran 2. Skema Modifikasi Silika Mesopori MCM-41 dengan Zn

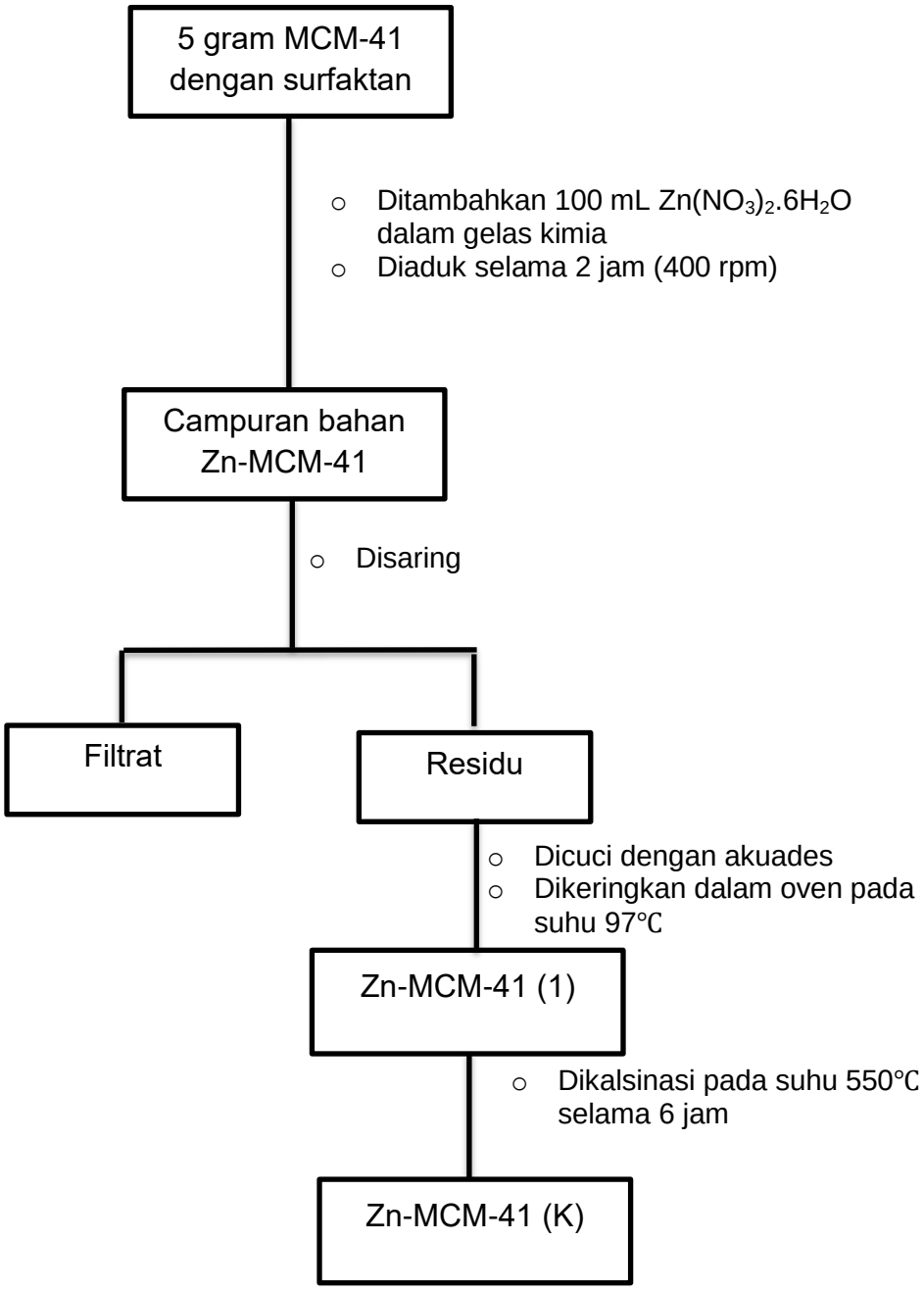

Lampiran 3. Pembuatan Larutan Induk MK dan BBR

a. Zat Warna MK

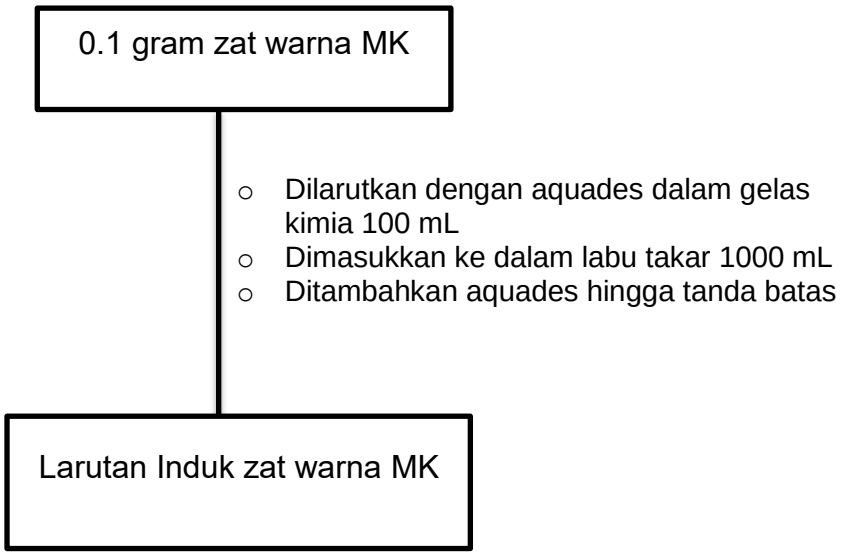

b. Zat Warna BCR

Lampiran 4. Penentuan Panjang Gelombang Maksimum

a. Zat warna MK

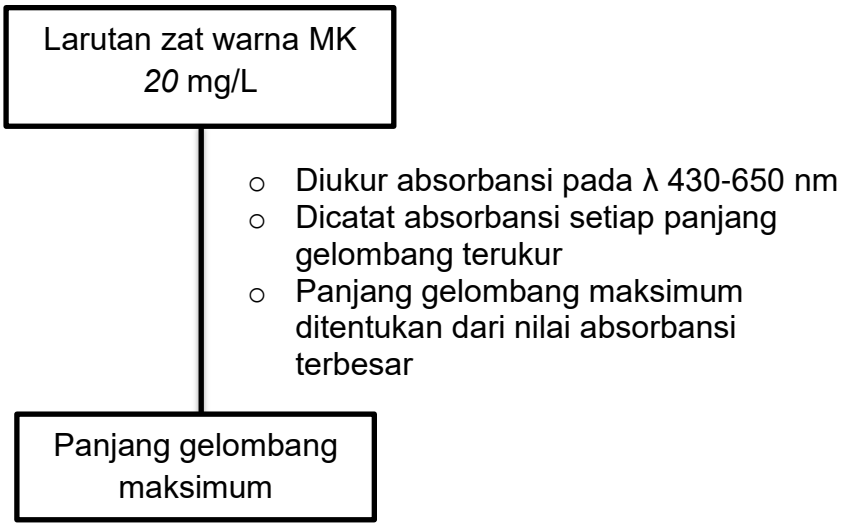

b. Zat warna BCR

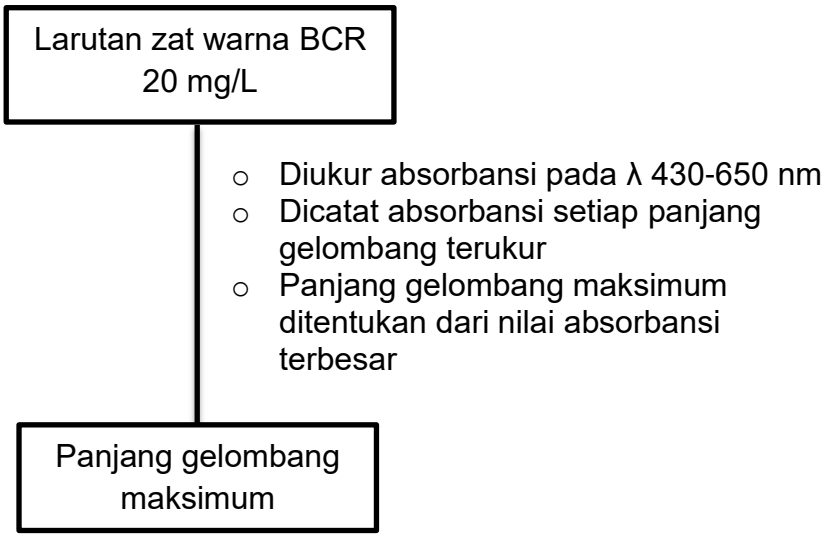

Lampiran 5. Pembuatan Kurva Kalibrasi Larutan Standar Zat Warna MK dan BCR

a. Zat warna MK

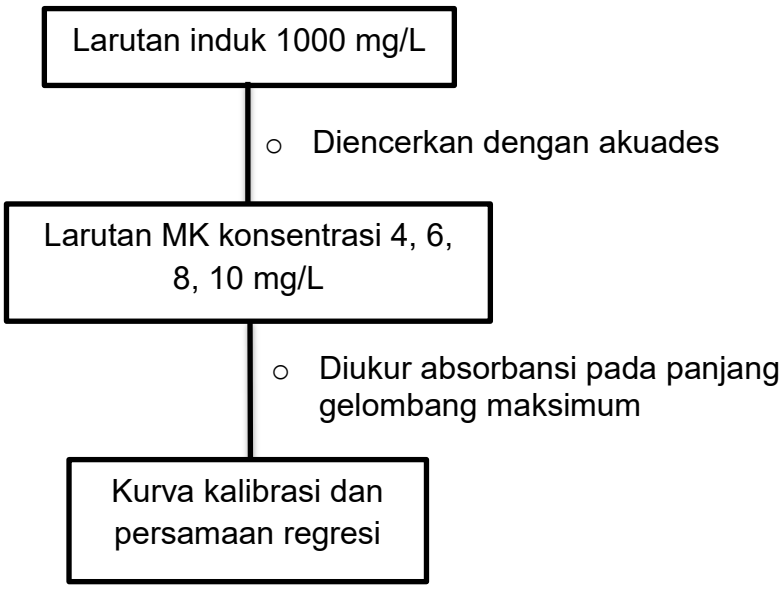

b. Zat warna BCR

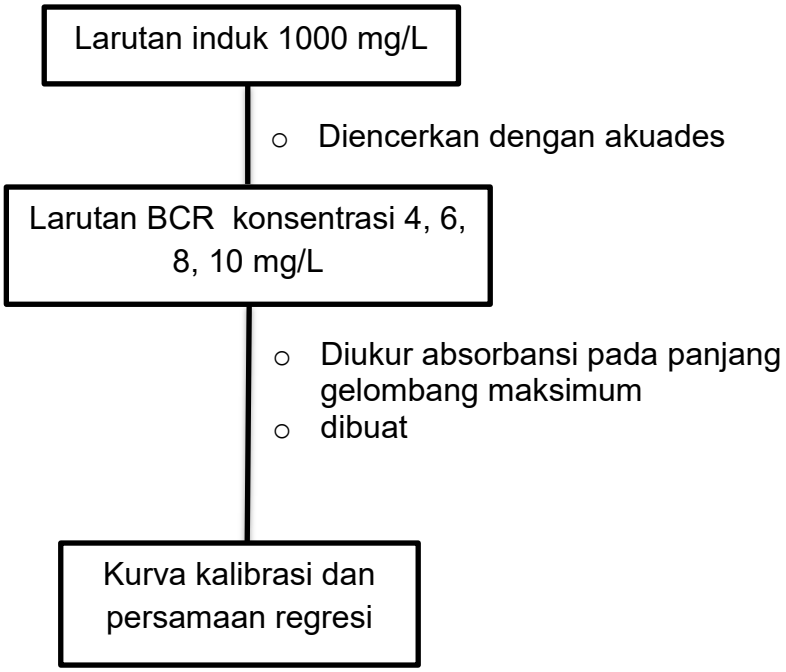

Lampiran 6. Penentuan Waktu Kontak Optimum

a. Zat warna MK

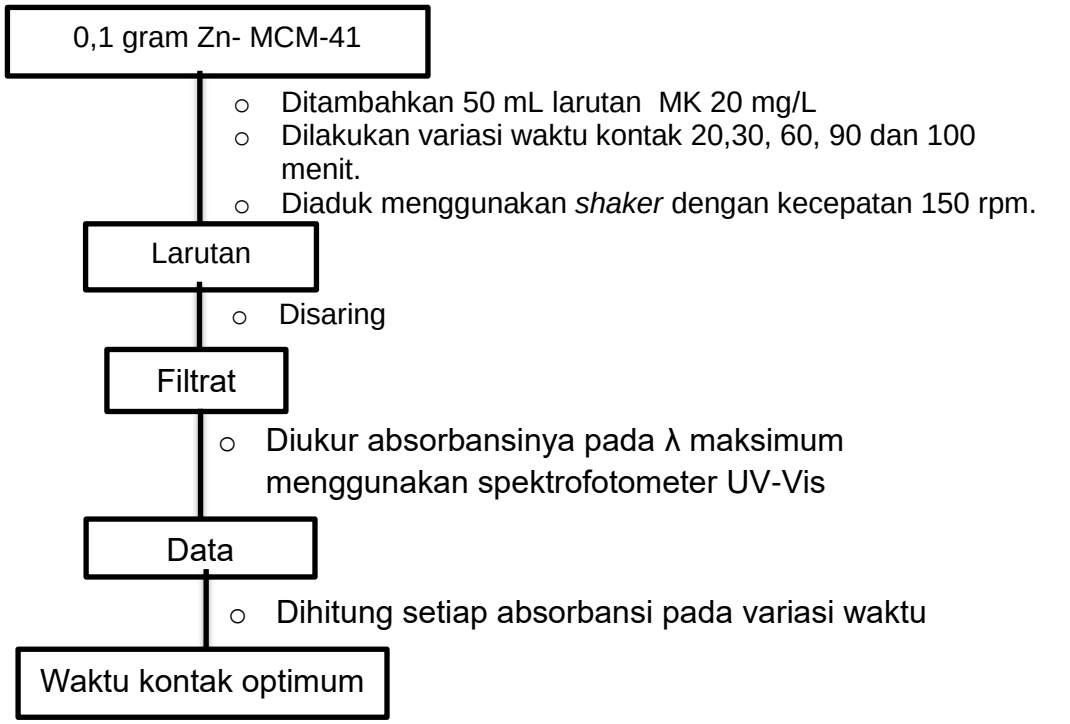

b. Zat warna BCR

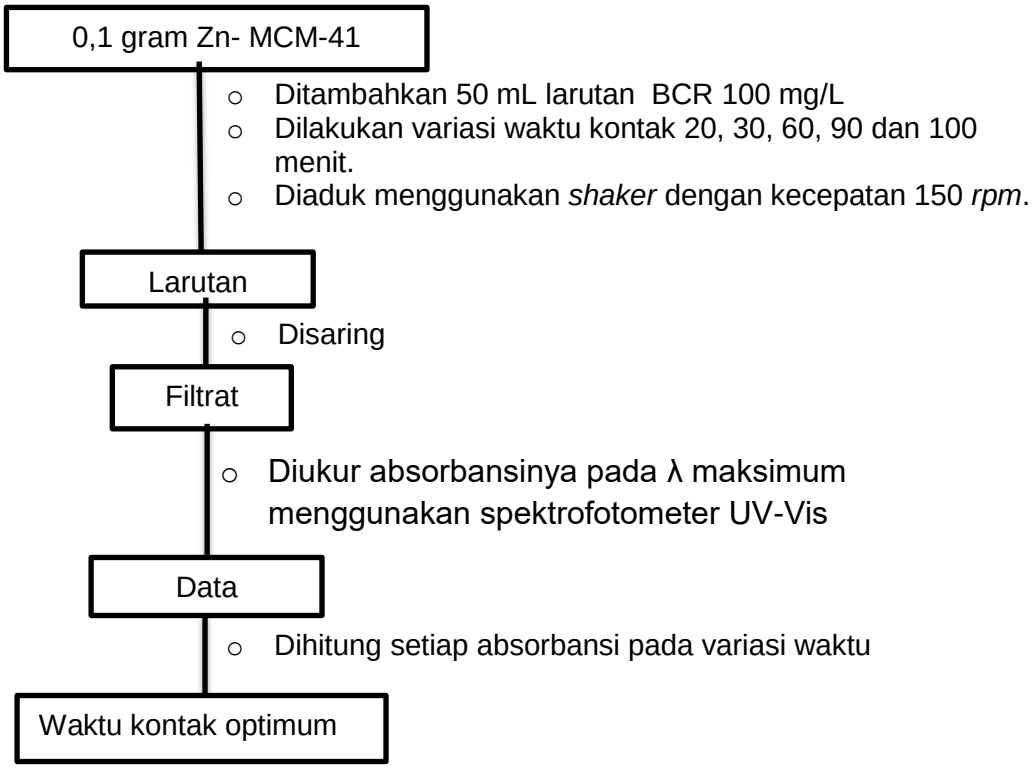

Lampiran 7. Penentuan Kapasitas Adsorpsi

a. Zat warna MK

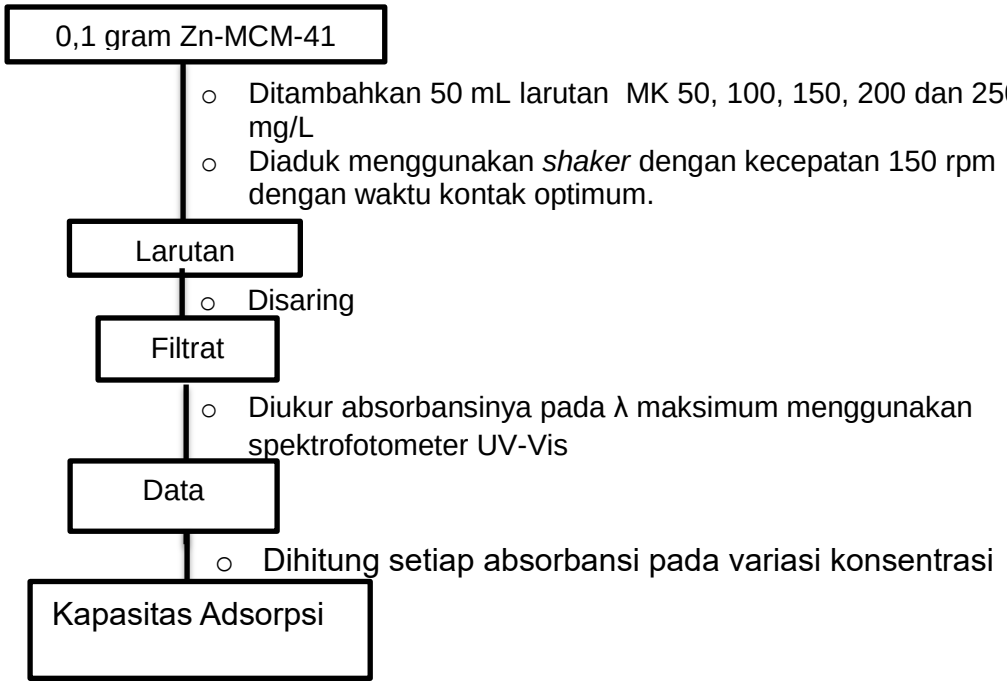

b. Zat Warna BCR

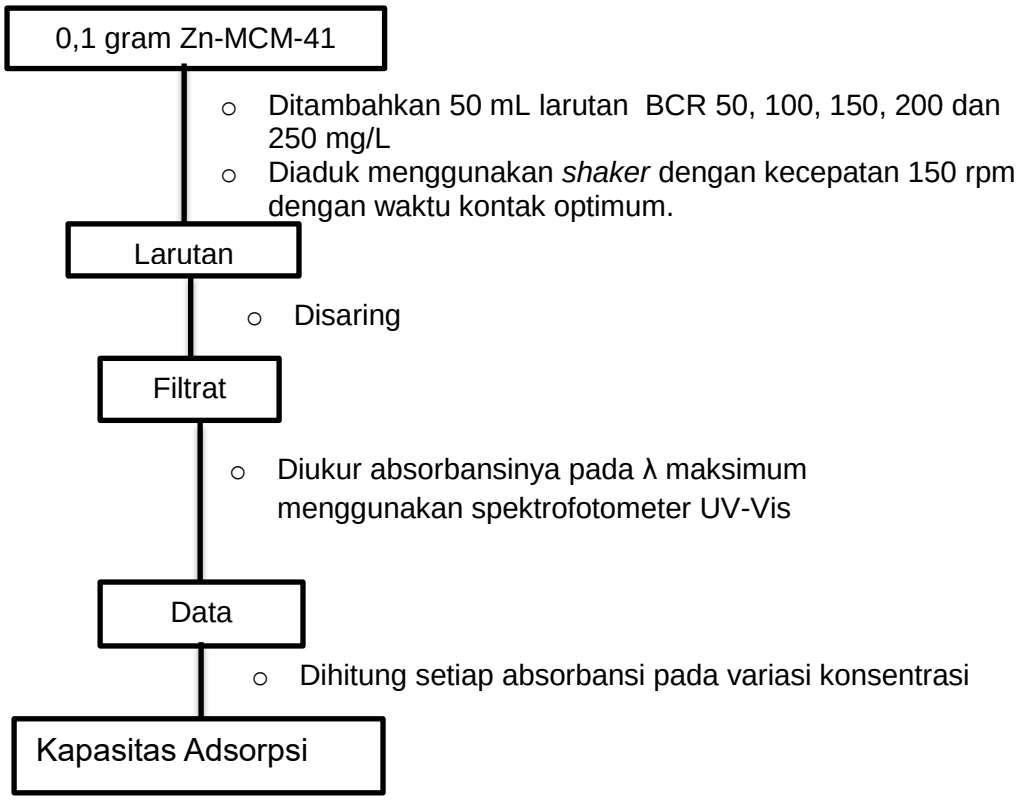

Lampiran 8. Desorpsi MK dan BCR dari Zn-MCM-41

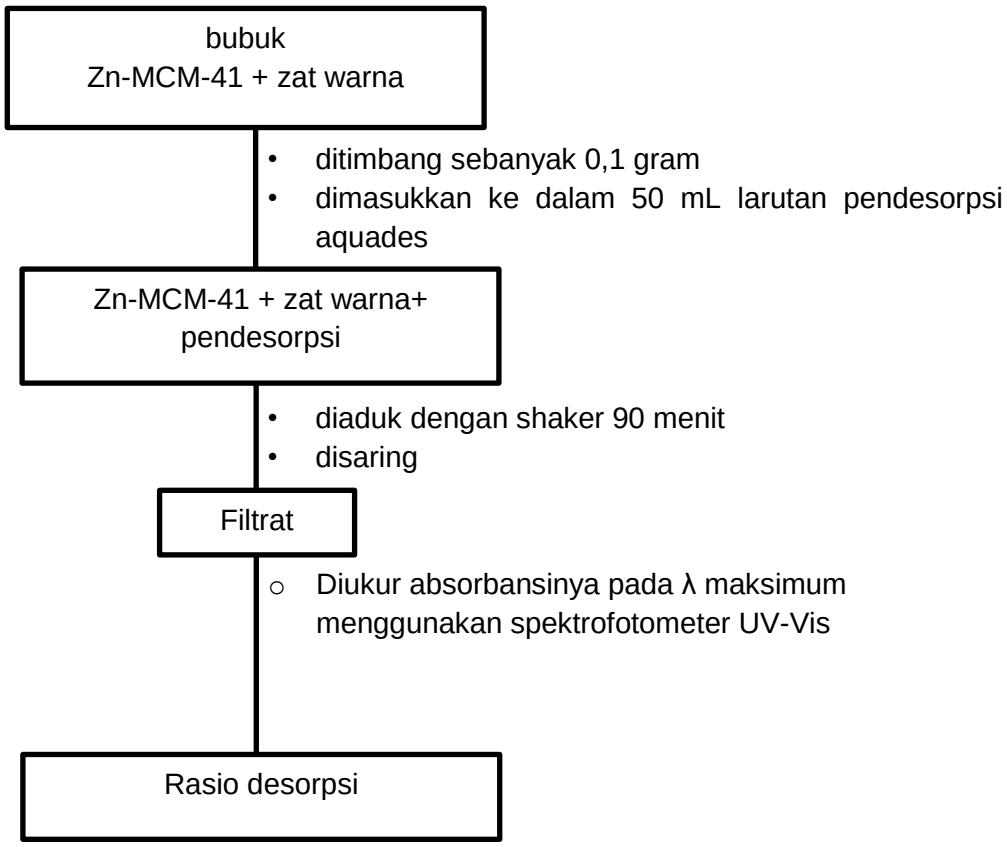

Lampiran 9. Panjang Gelombang Maksimum dan Kurva Kalibrasi Larutan Standar Zat Warna MK

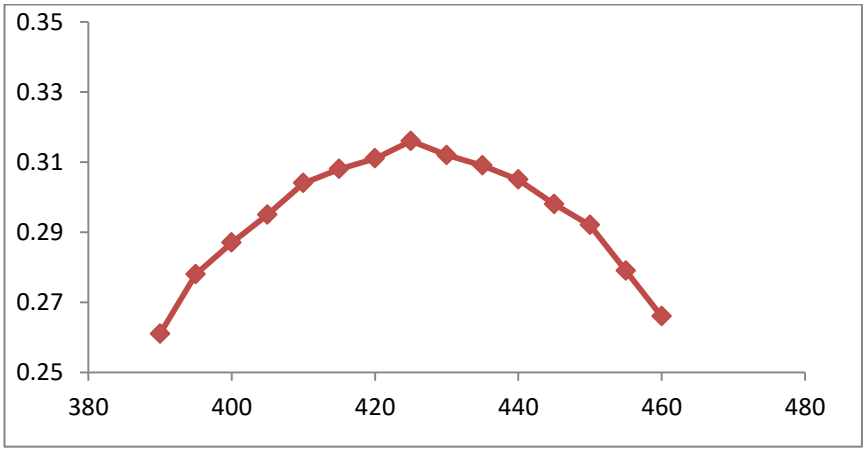

Gambar 27. Panjang gelombang maksimum MK

Lampiran 10. Data penentuan waktu optimum dan kinetika adsorpsi MK oleh MCM-41 dan Zn-MCM-41

Tabel 8. Data penentuan waktu optimum MK oleh MCM-41

Waktu (menit)	Adsorben (gram)	C_0 (mg/L)	Ce (mg/L)	qt (mg/g)
5	0.1004	20.4552	17.4220	1.5106
10	0.1004	20.4552	17.3116	1.5655
15	0.1004	20.4552	16.6612	1.8894
25	0.1004	20.4552	16.8780	1.7815
35	0.1002	20.4552	16.9864	1.7309
45	0.1003	20.4552	17.0948	1.6752
60	0.1004	20.4552	17.2032	1.6195
90	0.1002	20.4552	17.3116	1.5687

Tabel 9. Data studi kinetika adsorpsi MK oleh MCM-41

Waktu (menit)	qe (mg/g)	qt (mg/g)	qe-qt	ln (qe-qt)	t/qt (g/mg.menit)
5	1.8894	1.5106	0.3789	-0.9705	3.3100
10	1.8894	1.5655	0.3239	-1.1273	6.3876
15	1.8894	1.8894	0.0000	0.0000	7.9389
25	1.8894	1.7815	0.1080	-2.2259	14.0333
35	1.8894	1.7309	0.1585	-1.8420	20.2202
45	1.8894	1.6752	0.2143	-1.5405	26.8629
60	1.8894	1.6195	0.2699	-1.3096	37.0480
90	1.8894	1.5687	0.3208	-1.1370	57.3737

Tabel 10. Data penentuan waktu optimum MK oleh Zn-MCM-41

Waktu (menit)	Adsorben (gram)	C_0 (mg/L)	Ce (mg/L)	qt (mg/g)
5	0.1002	22.1084	9.4959	6.2936
10	0.1002	22.1084	9.4959	6.2936
15	0.1002	22.1084	9.4959	6.2936
25	0.1003	22.1084	9.4688	6.3009
35	0.1003	22.1084	9.3604	6.3549
45	0.1005	22.1084	9.4688	6.2883
60	0.1008	22.1084	9.6043	6.2024
90	0.1009	22.1084	9.6043	6.1963

Tabel 10. Data studi kinetika adsorpsi MK oleh Zn-MCM-41

Waktu (menit)	qe (mg/g)	qt (mg/g)	qe-qt	ln (qe-qt)	t/qt (g/mg.menit)
5	6.3549	6.2936	0.0613	-2.7924	0.7945
10	6.3549	6.2936	0.0613	-2.7924	1.5889
15	6.3549	6.2936	0.0613	-2.7924	2.3834
25	6.3549	6.3009	0.0540	-2.9181	3.9677
35	6.3549	6.3549	0.0000	0.0000	5.5075
45	6.3549	6.2883	0.0666	-2.7094	7.1561
60	6.3549	6.2024	0.1525	-1.8806	9.6737
90	6.3549	6.1963	0.1587	-1.8410	14.5249

Contoh perhitungan jumlah MK yang teradsorpsi (waktu = 35 menit):

$$q_t = \frac{(22{,}1084 - 9{,}3604)\text{mg/L}}{0{,}1003\text{ g}} \text{ x } 0{,}05 \text{ L}$$

$q_t = 6{,}3549$ mg/g

Contoh perhitungan nilai parameter kinetika orde satu semu.

Data grafik kinetika orde satu semu diperoleh persamaan garis :

y = 0.0129x - 2.6745

dari persamaan garis diperoleh nilai slope (a) = 0,0129 dan nilai intersep (b) = -2,6745

Nilai k_1 dapat dihitung sebagai berikut :

slope = *k*

k_1 = slope

= 0,0129 menit^{-1}

Nilai adsorpsi dapat dihitung sebagai berikut :

intersep = ln q_e

$q_e = e^{\text{intersep}}$

$= e^{-2{,}6745}$

= 0,0689 mg/g

Perhitungan nilai parameter kinetika orde dua semu adalah sebagai berikut.

Data grafik kinetika orde dua semu diperoleh persamaan garis :

y = 0.1616x - 0.0583

dari persamaan garis diperoleh nilai slope (a) = 0,1616 dan nilai intersep (b) = 0,0583

Nilai adsorpsi dapat dihitung sebagai berikut :

$$\text{slope} = \frac{1}{q_e}$$

$$q_e = \frac{1}{\text{slope}} = \frac{1}{0{,}1616} = 6{,}1881 \text{ mg g}^{-1}$$

Nilai k_2 dapat dihitung sebagai berikut :

$$\text{intersep} = \frac{1}{k_2 . q_e^2}$$

$$k_2 = \frac{1}{q_e^2 . \text{intersep}}$$

$$= \frac{1}{(6{,}1881)^2 \text{ x } (0{,}0583)}$$

$$= 0{,}4479 \text{ g·mg}^{-1}\text{menit}^{-1}$$

Lampiran 11. Data penentuan Kapasitas dan Isotherm adsorpsi MK oleh MCM-41 dan Zn-MCM-41

Tabel 11. Data Penentuan Kapasitas Adsorpsi MK oleh MCM-41

Adsorben (gram)	Co (mg/L)	Ce (mg/L)	qe (mg/g)	Ce/qe	Log Ce	Log qe
0.1003	22.0813	15.3225	3.3693	4.5477	1.1853	0.5275
0.1003	34.0650	21.6911	6.1685	3.5164	1.3363	0.7902
0.1005	56.2873	31.6260	12.2693	2.5777	1.5000	1.0888
0.1005	79.0515	57.3713	10.7862	5.3190	1.7587	1.0329
0.1006	109.3225	84.1192	12.5265	6.7153	1.9249	1.0978
0.1006	170.5691	131.0027	19.6652	6.6616	2.1173	1.2937
0.1008	279.3496	254.4173	12.3672	20.5720	2.4055	1.0923

Tabel 12. Data Penentuan Kapasitas Adsorpsi MK oleh Zn-MCM-41

Adsorben (gram)	Co (mg/L)	Ce (mg/L)	qe (mg/g)	Ce/qe	Log Ce	Log qe
0.1002	22.5149	8.1409	7.1726	1.1350	0.9107	0.8557
0.1002	33.7940	12.7480	10.5020	1.2139	1.1054	1.0213
0.1002	56.0163	36.7751	9.6014	3.8302	1.5656	0.9823
0.1007	79.3225	49.5122	14.8015	3.3451	1.6947	1.1703
0.1008	115.2846	88.7263	13.1737	6.7351	1.9481	1.1197
0.1009	170.5691	136.9648	16.6523	8.2250	2.1366	1.2215
0.1011	285.8537	227.8591	28.6818	7.9444	2.3577	1.4576

Contoh perhitungan jumlah MK yang teradsorpsi (C_o = 22,5149mg/L) :

$$q_e = \frac{(22,5149 - 8,1409)\text{mg/L}}{0,1002\text{ g}} \text{ x } 0,05\text{ L}$$

q_e = 7,1726 mg/g

Perhitungan nilai parameter isotermal adsorpsi Langmuir sebagai berikut. Berdasarkan model isotermal Langmuir diperoleh persamaan garis :

y = 0.0571x + 0.9107

dari persamaan garis diperoleh nilai slope (a) = 0,0571 dan nilai intersep (b) = 0,9107

Nilai kapasitas adsorpsi dapat dihitung sebagai berikut :

$$\frac{1}{Q_0} = \text{slope}$$

$$Q_0 = \frac{1}{0,0571}$$

= 17,5131 mg/g

Intensitas adsorpsi dapat dihitung sebagai berikut :

$$\frac{1}{Q_0 . b} = \text{intersep}$$

$$b = \frac{1}{17,5131\text{ mg/g x } 0,9107} = 0,0627\text{ L mg}^{-1}$$

Perhitungan nilai parameter isotermal Freundlich sebagai berikut: Berdasarkan model isotermal Freundlich diperoleh persamaan garis :

y = 0.3294x + 0.5670

dari persamaan garis diperoleh nilai slope (a) = 0,3294 dan nilai intersep (b) = 0,5670

Nilai kapasitas adsorpsi dapat dihitung sebagai berikut :

log k_f = intersep

log k_f = 0,5670

k_f = 3,6897 mg/g

Intensitas adsorpsi dapat dihitung sebagai berikut :

$$\frac{1}{n} = \text{slope}$$

$$n = \frac{1}{\text{slope}} = \frac{1}{0,3294} = 3,0358\text{ g L}^{-1}$$

Lampiran 12. Panjang Gelombang Maksimum dan Kurva Kalibrasi Larutan Standar Zat Warna BCR

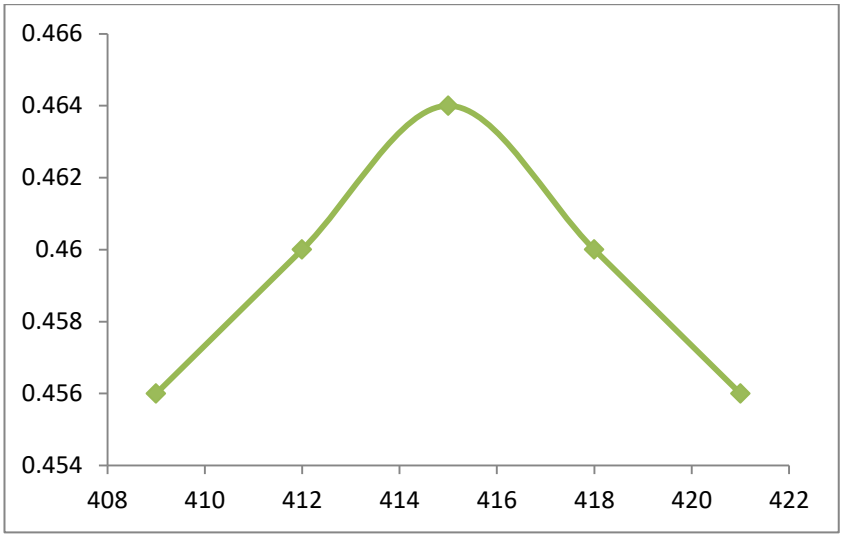

Gambar 28. Panjang gelombang maksimum BCR

Lampiran 13. Data Waktu Kontak Optimum dan Kinetika Adsorpsi BCR oleh MCM-41 dan Zn-MCM-41

Tabel 13. Data penentuan waktu optimum adsorpsi BCR oleh MCM-41

Waktu (menit)	Adsorben (gram)	C_0 (mg/L)	Ce (mg/L)	qt (mg/g)
5	0.1005	104.0264	25.4917	39.0720
10	0.1005	104.0264	23.8416	39.8929
15	0.1005	104.0264	22.1914	40.7139
20	0.1009	104.0264	20.3432	41.4684
30	0.1008	104.0264	19.7492	41.8042
45	0.1009	104.0264	18.4290	42.4169
60	0.1009	104.0264	17.8350	42.7113
90	0.1005	104.0264	18.6931	42.4544
120	0.1002	104.0264	19.3531	42.2521

Tabel 14. Data studi kinetika adsorpsi BCR oleh MCM-41

Waktu (menit)	qe (mg/g)	qt (mg/g)	qe-qt	ln (qe-qt)	t/qt (g/mg.menit)
5	42.7113	39.0720	3.6393	1.2918	0.1280
10	42.7113	39.8929	2.8184	1.0362	0.2507
15	42.7113	40.7139	1.9974	0.6918	0.3684
20	42.7113	41.4684	1.2429	0.2175	0.4823
30	42.7113	41.8042	0.9071	-0.0975	0.7176
45	42.7113	42.4169	0.2944	-1.2229	1.0609
60	42.7113	42.7113	0.0000	0.0000	1.4048
90	42.7113	42.4544	0.2569	-1.3590	2.1199
120	42.7113	42.2521	0.4592	-0.7783	2.8401

Tabel 15. Data penentuan waktu optimum adsorpsi BCR oleh Zn-MCM-41

Waktu (menit)	Adsorben (gram)	C_0 (mg/L)	Ce (mg/L)	qt (mg/g)
5	0.1002	101.1324	7.5436	46.7010
15	0.1003	101.1324	5.5226	47.6619
30	0.1004	101.1324	4.9303	47.9094
60	0.1005	101.1324	4.4774	48.0871
100	0.1005	101.1324	2.7352	48.9538
160	0.1004	101.1324	2.1429	49.2976
250	0.1005	101.1324	1.2718	49.6819
350	0.1002	101.1324	1.7247	49.6046
450	0.1013	101.1324	1.8293	49.0144

Tabel 16. Data studi kinetika adsorpsi BCR oleh Zn-MCM-41

Waktu (menit)	qe (mg/g)	qt (mg/g)	qe-qt	ln (qe-qt)	t/qt (g/mg.menit)
5	49.6819	46.7010	2.9809	1.0922	0.1071
15	49.6819	47.6619	2.0200	0.7031	0.3147
30	49.6819	47.9094	1.7725	0.5724	0.6262
60	49.6819	48.0871	1.5948	0.4668	1.2477
100	49.6819	48.9538	0.7281	-0.3174	2.0427
160	49.6819	49.2976	0.3843	-0.9563	3.2456
250	49.6819	49.6819	0.0000	0.0000	5.0320
350	49.6819	49.6046	0.0773	-2.5603	7.0558
450	49.6819	49.0144	0.6675	-0.4042	9.1810

Contoh perhitungan jumlah BCR yang teradsorpsi (waktu = 250 menit):

$$q_t = \frac{(101{,}1324 - 1{,}2718)\text{mg/L}}{0{,}1005\text{ g}} \text{ x } 0{,}05\text{ L}$$

q_t = 49,6819 mg/g

Contoh perhitungan nilai parameter kinetika orde satu semu.

Data grafik kinetika orde satu semu diperoleh persamaan garis :

$y = -0.0048x + 0.6028$

dari persamaan garis diperoleh nilai slope (a) = -0,0048 dan nilai intersep (b) = 0,6028

Nilai k_1 dapat dihitung sebagai berikut :

slope = $-k$

k_1 = - slope

= - (-0,0048)

= 0,0048 menit^{-1}

Nilai adsorpsi dapat dihitung sebagai berikut :

intersep = ln q_e

q_e = $e^{intersep}$

= $e^{0,6028}$

= 1,8272 mg/g

Perhitungan nilai parameter kinetika orde dua semu adalah sebagai berikut.

Data grafik kinetika orde dua semu diperoleh persamaan garis :

$y = 0.0203x + 0.0093$

dari persamaan garis diperoleh nilai slope (a) = 0,0203 dan nilai intersep (b) = 0,0093

Nilai adsorpsi dapat dihitung sebagai berikut :

slope = $\frac{1}{q_e}$

$q_e = \frac{1}{slope} = \frac{1}{0,0203}$ = 49,2611 mg g^{-1}

Nilai k_2 dapat dihitung sebagai berikut :

intersep = $\frac{1}{k_2 . q_e^2}$

$k_2 = \frac{1}{q_e^2 . intersep}$

$= \frac{1}{(49,2611)^2 \text{ x } (0,0093)}$

= 0,0443 g·mg^{-1}menit^{-1}

Lampiran 14. Penentuan kapasitas dan isothermal adsoprsi BCR oleh MCM-41 dan Zn-MCM-41

Tabel 17. Data Penentuan Kapasitas Adsorpsi BCR oleh MCM-41

Adsorben (gram)	Co (mg/L)	Ce (mg/L)	qe (mg/g)	Ce/qe	Log Ce	Log qe
0.1012	75.9736	7.4719	33.8447	0.2208	0.8734	1.5295
0.1006	102.7063	20.2772	40.9687	0.4949	1.3070	1.6125
0.1013	126.4686	42.3102	41.5392	1.0186	1.6264	1.6185
0.1016	152.2112	56.6667	47.0200	1.2052	1.7533	1.6723
0.1002	201.7822	104.3564	48.6156	2.1466	2.0185	1.6868
0.1005	252.2772	155.2475	48.2735	3.2160	2.1910	1.6837
0.1012	303.1023	209.7030	46.1459	4.5443	2.3216	1.6641

Tabel 18. Data Penentuan Kapasitas Adsorpsi BCR oleh Zn-MCM-41

Adsorben (gram)	Co (mg/L)	Ce (mg/L)	Qe (mg/g)	Ce/qe	Log Ce	Log qe
0.1007	101.2195	1.0976	49.713	0.0221	0.0404	1.6965
0.1015	126.3066	1.6899	61.387	0.0275	0.2279	1.7881
0.1004	151.3937	3.7805	73.512	0.0514	0.5775	1.8664
0.1005	207.4913	6.8467	99.823	0.0686	0.8355	1.9992
0.1013	255.4007	18.1359	117.110	0.1549	1.2585	2.0686
0.1016	308.7108	27.2648	138.506	0.1968	1.4356	2.1415
0.1013	404.5296	93.8153	153.363	0.6117	1.9723	2.1857

Contoh perhitungan jumlah BCR yang teradsorpsi (C_o = 101,2195 mg/L) :

$$q_e = \frac{(101{,}2195 - 1{,}0976)\text{mg/L}}{0{,}1007\text{ g}} \text{ x } 0{,}05 \text{ L}$$

q_e = 49,713 mg/g

Contoh perhitungan nilai parameter isotermal adsorpsi Langmuir sebagai berikut.

Berdasarkan model isotermal Langmuir diperoleh persamaan garis :

y = 0.0063x + 0.0247

dari persamaan garis diperoleh nilai slope (a) = 0,0063 dan nilai intersep (b) = 0,0247

Nilai kapasitas adsorpsi dapat dihitung sebagai berikut :

$$\frac{1}{Q_0} = \text{slope}$$

$$Q_0 = \frac{1}{0{,}0063} = 158{,}7302 \text{ mg/g}$$

Intensitas adsorpsi dapat dihitung sebagai berikut :

$\frac{1}{Q_0 . b}$ = intersep

$b = \frac{1}{158{,}7302 \text{ mg/g x } 0{,}0247} = 0{,}2551 \text{ L mg}^{-1}$

Contoh perhitungan nilai parameter isotermal Freundlich sebagai berikut:

Berdasarkan model isotermal Freundlich diperoleh persamaan garis :

$y = 0.2611x + 1.7269$

dari persamaan garis diperoleh nilai slope (a) = 0,2611 dan nilai intersep (b) = 1,7269

Nilai kapasitas adsorpsi dapat dihitung sebagai berikut :

log k_f = intersep

log k_f = 1,7269

k_f = 53,3212 mg/g

Intensitas adsorpsi dapat dihitung sebagai berikut :

$\frac{1}{n}$ = slope

$n = \frac{1}{\text{slope}} = \frac{1}{0{,}2611} = 3{,}8300 \text{ g L}^{-1}$

Lampiran 15. Penentuan Desorpsi MK dan BCR oleh MCM-41 dan Zn-MCM-41

Tabel 19. Data penentuan % Rasio Desorpsi MK dan BCR

Sampel	qe adsorpsi (mg/g)	C desorpsi (mg/L)	V (L)	Wa (gram)	qe desorpsi (mg/g)	Rasio desorpsi (%)
MCM-41/ MK	4.3307	5.2412	0.05	0.1009	2.5972	59.9719
Zn-MCM-41/ MK	5.0517	3.0732	0.05	0.1012	1.5184	30.0565
MCM-41/ BCR	23.2173	3.8850	0.05	0.1023	1.8988	8.1785
Zn-MCM-41/BCR	26.5423	6.9512	0.05	0.1024	3.3942	12.7876

Contoh perhitungan % rasio desorpsi MK dari MCM-41

$$\% \text{ Rasio desorpsi} = \frac{2{,}5972}{4{,}3307} \times 100\%$$

$$= 59{,}9719\%$$

Lampiran 16. Hasil XRD

Match! Phase Analysis Report

Sample: MCM-41-K (2-80)

Sample Data

File name	MCM-41-K.RAW
File path	F:/
Data collected	Jun 9, 2022 14:24:33
Data range	2.000° - 80.000°
Original data range	2.000° - 80.000°
Number of points	7801
Step size	0.010
Rietveld refinement converged	No
Alpha2 subtracted	No
Background subtr.	No
Data smoothed	No
Radiation	X-rays
Wavelength	1.540600 Å

Peak List

No.	2theta [°]	d [Å]	I/I0 (peak height)	Counts (peak area)	FWHM
1	2.29	38.5484	0.31	0.10	1.7300
2	3.81	23.1722	158.21	51.42	1.7300
3	4.57	19.3202	78.49	135.00	1.7300
4	5.71	15.4652	606.20	197.00	1.7300
5	7.33	12.0505	16.51	56.79	3.4600
6	9.61	9.1960	189.83	226.27	6.3455
7	22.45	3.9571	1000.00	1524.00	8.1130
8	57.65	1.5977	155.54	101.09	3.4600
9	64.59	1.4418	148.24	204.84	7.3559
10	69.06	1.3589	180.78	117.50	3.4600
11	77.72	1.2277	201.82	131.18	3.4600

Integrated Profile Areas

Based on calculated profile

Profile area	Counts	Amount
Overall diffraction profile	1454508	100.00%
Background radiation	1170163	80.45%
Diffraction peaks	284345	19.55%
Peak area belonging to selected phases	0	0.00%
Unidentified peak area	284345	19.55%

Peak Residuals

Peak data	Counts	Amount
Overall peak intensity	2745	100.00%
Peak intensity belonging to selected phases	0	0.00%
Unidentified peak intensity	2745	100.00%

Diffraction Pattern Graphics

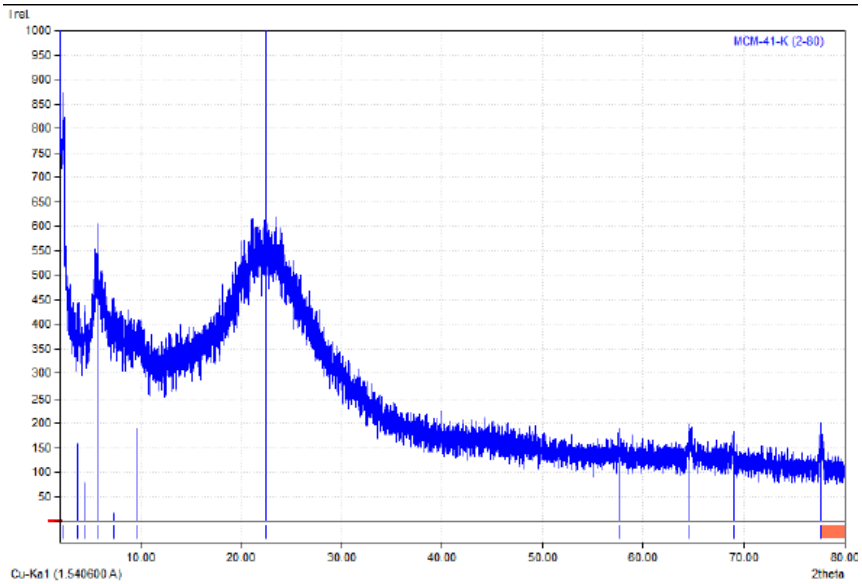

Match! Phase Analysis Report

Sample: Zn-MCM-41_K (2-80)

Sample Data

File name	Zn-MCM-41_K.RAW
File path	F:/
Data collected	Jun 9, 2022 14:24:26
Data range	2.000° - 80.000°
Original data range	2.000° - 80.000°
Number of points	7801
Step size	0.010
Rietveld refinement converged	No
Alpha2 subtracted	No
Background subtr.	No
Data smoothed	Yes
Radiation	X-rays
Wavelength	1.540600 Å

Peak List

No.	*2theta [°]*	*d [Å]*	*I/I0 (peak height)*	*Counts (peak area)*	*FWHM*
1	2.38	37.0909	1000.00	20.70	0.1786
2	3.90	22.6377	240.10	6.35	0.2282
3	4.47	19.7522	145.94	4.40	0.2602
4	5.80	15.2254	216.53	7.33	0.2921
5	7.61	11.6077	153.05	1.84	0.1035
6	8.75	10.0978	33.76	0.18	0.0459
7	9.32	9.4815	12.90	0.10	0.0669
8	10.47	8.4425	21.29	0.10	0.0405
9	22.83	3.8921	588.45	5.45	0.0800
10	63.07	1.4728	82.56	0.77	0.0800
11	64.69	1.4398	129.99	4.24	0.2815
12	77.72	1.2277	130.32	4.25	0.2815

Integrated Profile Areas

Based on calculated profile

Profile area	*Counts*	*Amount*
Overall diffraction profile	239901	100.00%
Background radiation	174767	72.85%
Diffraction peaks	65133	27.15%
Peak area belonging to selected phases	0	0.00%
Unidentified peak area	65133	27.15%

Peak Residuals

Peak data	*Counts*	*Amount*
Overall peak intensity	56	100.00%
Peak intensity belonging to selected phases	45	81.49%
Unidentified peak intensity	10	18.51%

Diffraction Pattern Graphics

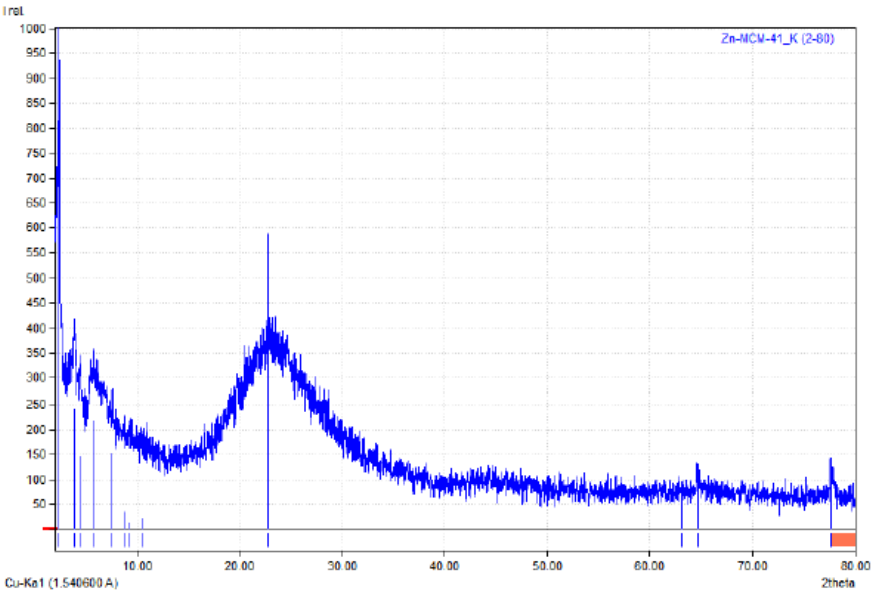

Lampiran 17. Hasil FTIR

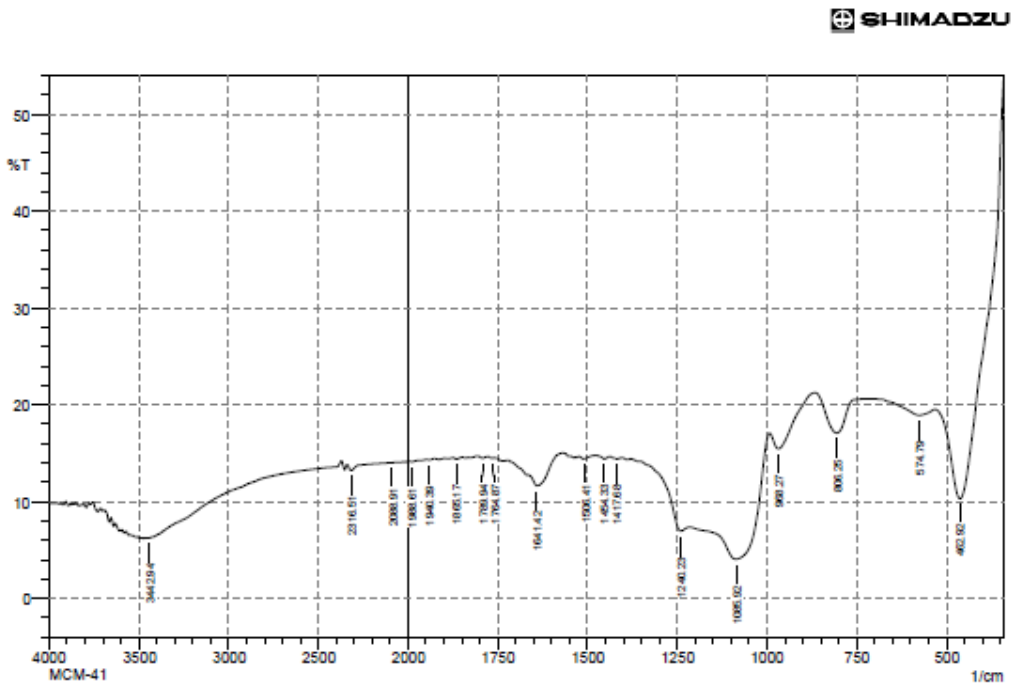

No.	Peak	Intensity	Corr. Intensity	Base (H)	Base (L)	Area	Corr. Area
1	462.92	10.303	21.483	530.42	339.47	132.782	40.079
2	574.79	18.921	0.846	721.38	532.35	132.929	1.199
3	806.25	17.08	3.909	866.04	723.31	101.992	5.045
4	968.27	15.442	2.389	991.41	867.97	91.736	2.977
5	1085.92	4.051	8.916	1213.23	993.34	259.214	50.488
6	1240.23	6.953	1.634	1354.03	1215.15	135.795	2.02
7	1417.68	14.386	0.189	1436.97	1406.11	25.895	0.095
8	1454.33	14.4	0.289	1465.9	1438.9	22.621	0.124
9	1506.41	14.416	0.047	1508.33	1485.19	19.335	0.008
10	1641.42	11.63	1.646	1662.64	1570.06	81.761	2.405
11	1764.87	14.487	0.07	1776.44	1761.01	12.926	0.024
12	1789.94	14.496	0.184	1805.37	1778.37	22.578	0.078
13	1865.17	14.368	0.175	1874.81	1849.73	21.049	0.061
14	1940.39	14.3	0.065	1948.1	1926.89	17.888	0.019
15	1988.61	14.118	0.07	1998.25	1971.25	22.914	0.026
16	2088.91	14.014	0.005	2092.77	2071.55	18.098	0.001
17	2316.51	13.206	0.588	2337.72	2268.29	60.348	0.607
18	3442.94	6.222	0.057	3448.72	2403.3	1017.99	0.048

Comment;
MCM-41

Date/Time; 9/17/2021 3:36:41 PM
No. of Scans;
Resolution;
Apodization;

SHIMADZU

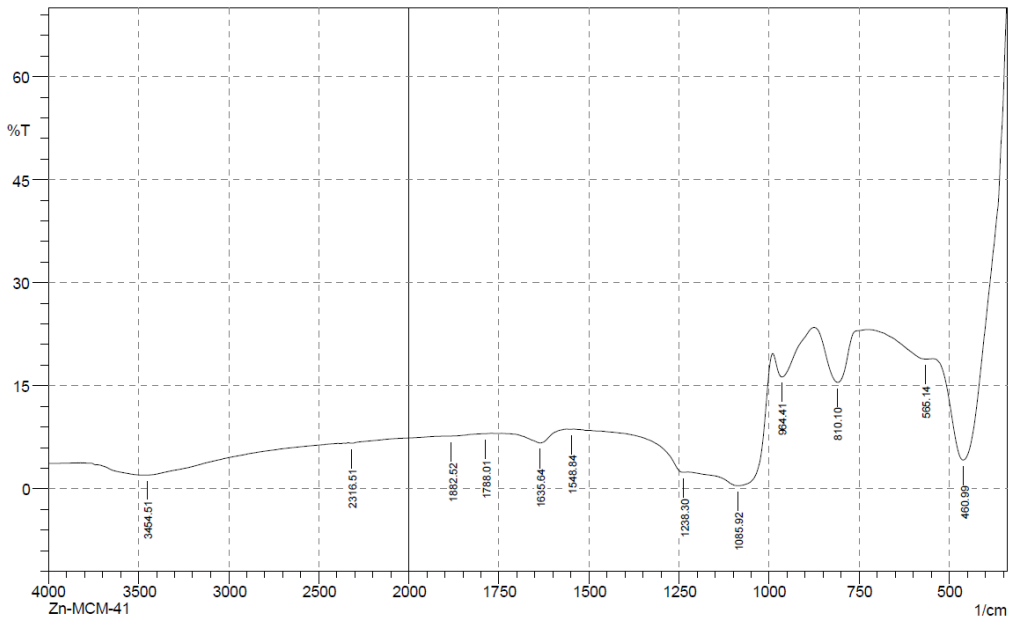

No.	Peak	Intensity	Corr. Intensity	Base (H)	Base (L)	Area	Corr. Area
1	460.99	4.17	36.204	543.93	339.47	165.377	77.334
2	565.14	18.881	0.512	725.23	545.85	121.784	0.686
3	810.1	15.483	7.871	873.75	727.16	102.975	10.323
4	964.41	16.27	4.248	989.48	875.68	80.784	4.902
5	1085.92	0.451	12.229	1224.8	991.41	405.343	135.259
6	1238.3	2.385	0.351	1442.75	1226.73	266.044	0.669
7	1548.84	8.637	0.013	1550.77	1543.05	8.201	0.003
8	1635.64	6.663	1.692	1718.58	1562.34	174.673	6.058
9	1788.01	8.005	0.006	1789.94	1770.65	21.117	0.003
10	1882.52	7.673	0.007	1884.45	1789.94	104.458	0.025
11	2316.51	6.613	0.119	2335.8	1888.31	511.838	0.286
12	3454.51	1.986	0.018	3458.37	2393.66	1448.618	0.167

Comment;
Zn-MCM-41

Date/Time; 9/21/2021 2:39:13 PM
No. of Scans;
Resolution;
Apodization;

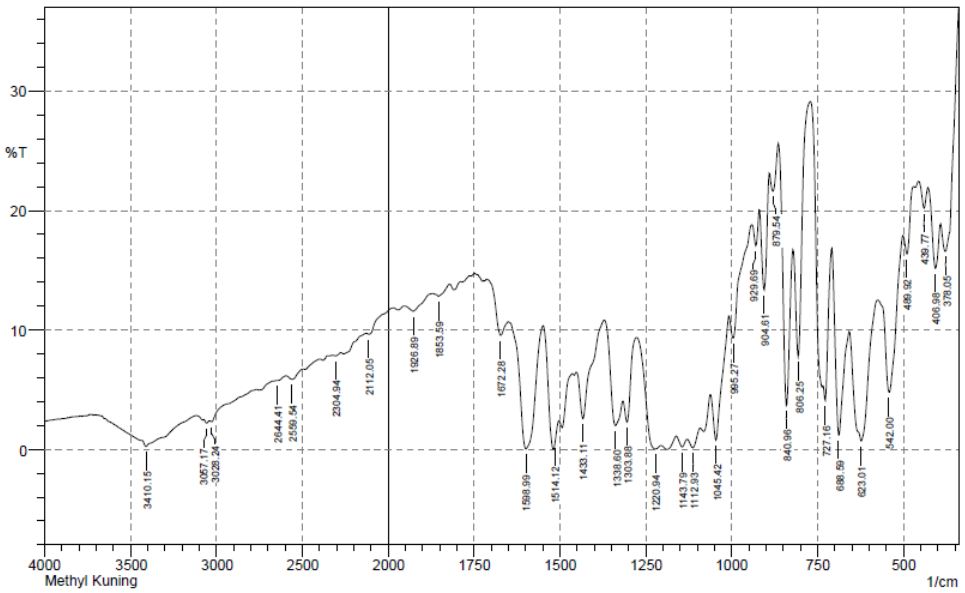

No.	Peak	Intensity	Corr. Intensity	Base (H)	Base (L)	Area	Corr. Area
1	378.05	16.591	6.991	391.55	339.47	34.429	4.611
2	406.98	15.18	4.871	426.27	393.48	24.768	1.972
3	439.77	20.194	1.964	455.2	428.2	18.146	0.493
4	489.92	16.375	3.083	501.49	470.63	22.541	0.998
5	542	4.793	10.061	572.86	503.42	70.643	13.411
6	623.01	0.689	10.227	655.8	574.79	113.317	36.053
7	688.59	1.187	12.988	707.88	657.73	63.175	18.364
8	727.16	4.076	4.083	732.95	709.8	24.817	1.794
9	806.25	7.773	12.339	819.75	771.53	36.638	5.657
10	840.96	3.676	17.107	864.11	821.68	40.811	11.627
11	879.54	21.637	2.576	891.11	864.11	17.28	0.718
12	904.61	13.34	8.25	918.12	891.11	20.859	2.911
13	929.69	17.06	2.37	939.33	920.05	14.305	0.604
14	995.27	9.322	3.146	1006.84	941.26	56.07	1.655
15	1045.42	0.77	5.772	1060.85	1008.77	73.204	13.952
16	1112.93	0.128	1.104	1128.36	1091.71	82.68	12.857
17	1143.79	0.202	0.755	1159.22	1130.29	67	8.478
18	1220.94	0.024	2.301	1274.95	1205.51	143.358	24.194
19	1303.88	2.278	3.368	1315.45	1276.88	50.187	4.413
20	1338.6	1.981	4.828	1369.46	1317.38	72.384	10.743
21	1433.11	2.579	4.831	1450.47	1371.39	94.65	9.693
22	1514.12	0.237	0.355	1516.05	1504.48	21.341	0
23	1598.99	0.025	10.493	1649.14	1548.84	153.647	55.531
24	1672.28	9.55	2.37	1712.79	1651.07	58.024	2.035
25	1853.59	12.821	0.505	1870.95	1820.8	44.126	0.441
26	1926.89	11.571	0.785	1953.89	1872.88	74.074	1.017
27	2112.05	9.649	0.305	2127.48	1984.75	138.012	0.428
28	2304.94	7.831	0.118	2318.44	2276	46.706	0.144
29	2559.54	5.867	0.494	2592.33	2497.82	114.161	1.646
30	2644.41	5.766	0.015	2646.34	2594.26	63.797	0.088
31	3028.24	2.313	0.204	3041.74	2767.85	386.739	0.429
32	3057.17	2.201	0.238	3072.6	3043.67	47.385	0.724
33	3410.15	0.228	2.584	3668.61	3116.97	1029.673	174.133

SHIMADZU

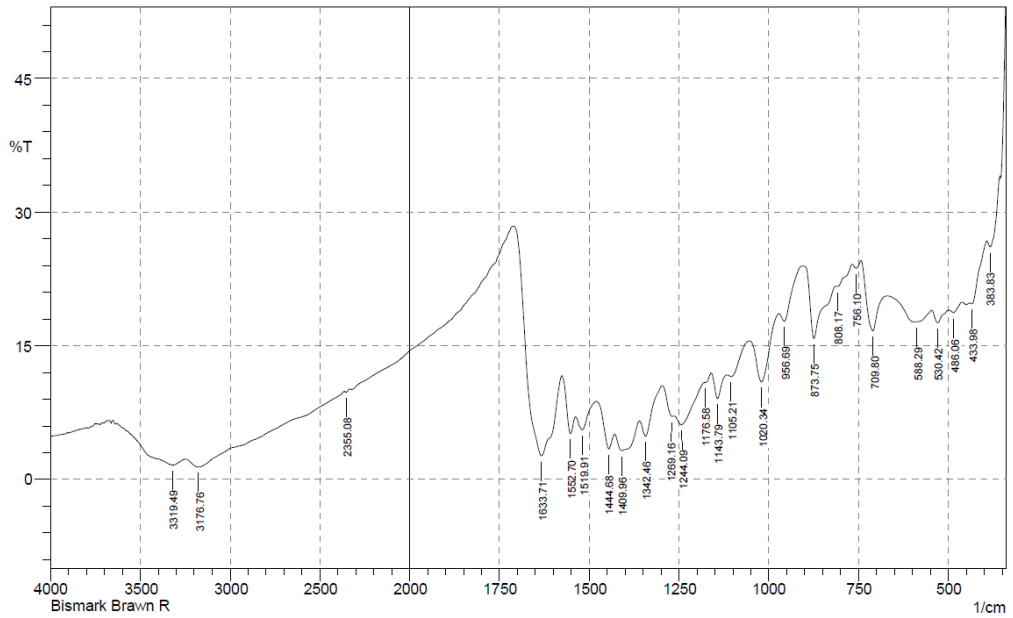

No.	Peak	Intensity	Corr. Intensity	Base (H)	Base (L)	Area	Corr. Area
1	383.83	26.065	2.597	393.48	356.83	20.136	1.062
2	433.98	19.703	0.957	439.77	393.48	29.656	0.322
3	486.06	18.706	0.586	497.63	462.92	24.92	0.244
4	530.42	17.58	1.414	545.85	499.56	34.1	0.71
5	588.29	17.69	0.058	590.22	547.78	31.446	0.196
6	709.8	16.658	6.067	742.59	671.23	50.766	4.428
7	756.1	23.706	0.634	767.67	742.59	15.538	0.157
8	808.17	21.635	0.344	813.96	767.67	29.887	0.233
9	873.75	15.812	7.326	906.54	813.96	65.298	5.789
10	956.69	17.738	2.02	970.19	908.47	42.429	0.936
11	1020.34	10.942	5.841	1053.13	972.12	68.542	6.291
12	1105.21	11.543	0.781	1114.86	1055.06	52.441	0.714
13	1143.79	9.07	2.779	1159.22	1116.78	41.467	2.105
14	1176.58	10.87	0.121	1178.51	1161.15	16.454	0.112
15	1244.09	6.129	1.836	1263.37	1178.51	93.535	4.154
16	1269.16	7.061	0.653	1296.16	1263.37	35.366	0.518
17	1342.46	4.847	2.808	1359.82	1296.16	72.263	3.836
18	1409.96	3.236	2.185	1427.32	1361.74	91.317	9.986
19	1444.68	3.417	2.79	1479.4	1429.25	63.592	4.553
20	1519.91	5.541	2.024	1537.27	1481.33	64.695	2.972
21	1552.7	5.14	3.554	1575.84	1539.2	41.786	3.311
22	1633.71	2.627	16.127	1708.93	1577.77	144.931	47.372
23	2355.08	9.775	0.18	2362.8	2337.72	25.176	0.119
24	3176.76	1.386	1.496	3248.13	2364.73	1187.685	29.561
25	3319.49	1.602	1.367	3597.24	3250.05	541.639	40.842

Comment;

Bismark Brawn R

Date/Time; 2/18/2022 10:41:44 AM

No. of Scans;

Resolution;

Apodization;

SHIMADZU

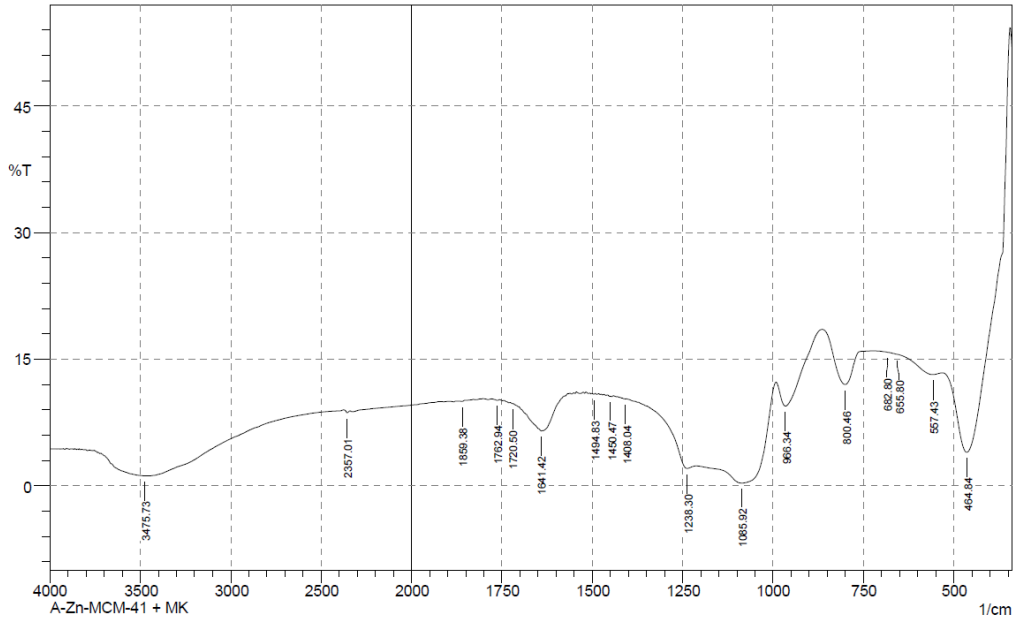

No.	Peak	Intensity	Corr. Intensity	Base (H)	Base (L)	Area	Corr. Area
1	464.84	3.967	24.154	532.35	345.26	171.049	64.466
2	557.43	13.168	0.661	653.87	532.35	103.329	1.166
3	655.8	15.565	0.019	680.87	653.87	21.726	0.007
4	682.8	15.812	0.017	723.31	680.87	33.855	-0.026
5	800.46	11.993	5.392	864.11	723.31	116.286	8.703
6	966.34	9.444	4.054	991.41	864.11	112.474	7.868
7	1085.92	0.331	7.707	1211.3	993.34	390.423	114.214
8	1238.3	2.048	1.35	1404.18	1213.23	232.228	3.326
9	1408.04	10.279	0.067	1421.54	1404.18	17.105	0.035
10	1450.47	10.597	0.041	1458.18	1448.54	9.378	0.012
11	1494.83	10.846	0.092	1500.62	1492.9	7.432	0.017
12	1641.42	6.486	0.21	1718.58	1637.56	88.548	-0.374
13	1720.5	9.723	0.047	1728.22	1718.58	9.734	0.006
14	1762.94	10.125	0.111	1778.37	1757.15	21.032	0.047
15	1859.38	9.993	0.114	1874.81	1851.66	23.106	0.05
16	2357.01	8.665	0.28	2374.37	2339.65	36.615	0.215
17	3475.73	1.172	0.027	3550.95	3468.01	157.762	1.097

Comment;

A-Zn-MCM-41 + MK

Date/Time; 4/27/2022 8:23:05 AM

No. of Scans;

Resolution;

Apodization;

SHIMADZU

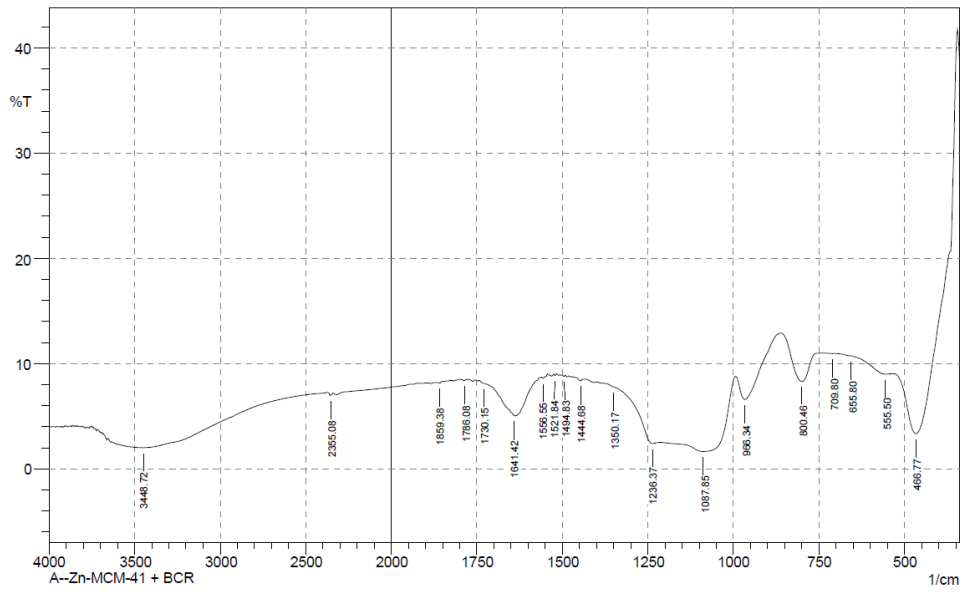

No.	Peak	Intensity	Corr. Intensity	Base (H)	Base (L)	Area	Corr. Area
1	466.77	3.345	17.401	534.28	345.26	196.062	61.636
2	555.5	8.999	0.348	653.87	534.28	121.024	0.687
3	655.8	10.733	0.018	680.87	653.87	26.102	0.025
4	709.8	10.958	0.017	738.74	700.16	37.006	0.008
5	800.46	8.312	3.647	862.18	738.74	122.093	8.071
6	966.34	6.591	3.051	993.34	862.18	135.855	8.306
7	1087.85	1.657	4.459	1213.23	995.27	349.179	60.334
8	1236.37	2.409	0.872	1371.39	1215.15	202.548	2.318
9	1350.17	7.787	0.027	1373.32	1348.24	27.57	0.005
10	1444.68	8.373	0.188	1458.18	1440.83	18.601	0.108
11	1494.83	8.781	0.11	1500.62	1490.97	10.159	0.024
12	1521.84	8.866	0.154	1525.69	1517.98	8.088	0.027
13	1556.55	8.608	0.143	1560.41	1550.77	10.245	0.045
14	1641.42	5.042	0.166	1718.58	1637.56	96.128	-0.674
15	1730.15	8.096	0.082	1745.58	1726.29	20.908	0.017
16	1786.08	8.39	0.112	1795.73	1776.44	20.696	0.048
17	1859.38	8.152	0.11	1869.02	1847.81	23.016	0.045
18	2355.08	6.982	0.255	2374.37	2339.65	39.829	0.243
19	3448.72	2.015	0.003	3456.44	3439.08	29.432	0.006

Comment;
A--Zn-MCM-41 + BCR

Date/Time; 4/27/2022 8:50:44 AM
No. of Scans;
Resolution;
Apodization;

Lampiran 18. Hasil SEM-EDS

View002

JEOL 1/1

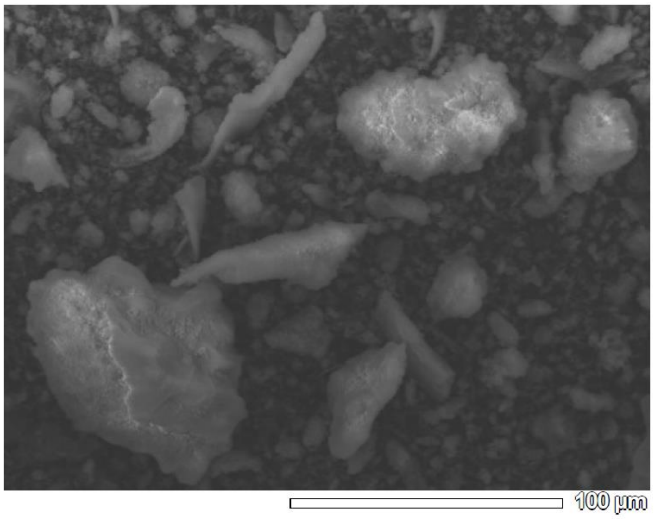

Title	: IMG1
Instrument	: JCM-6000PLUS
Volt	: 15.00 kV
Mag.	: x 500
Date	: 2022/04/01
Pixel	: 512 x 384

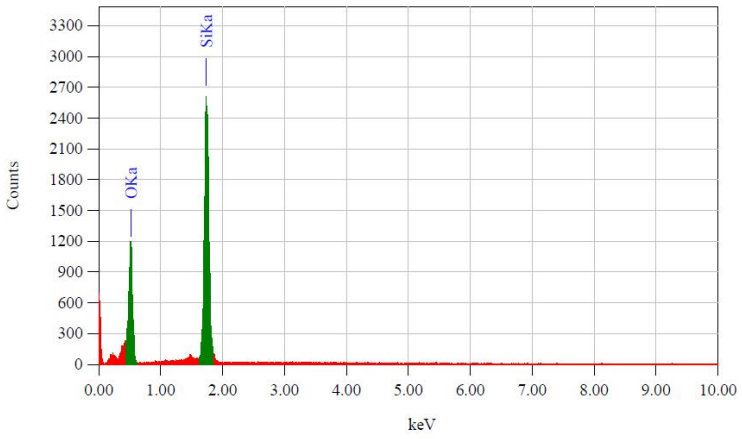

Acquisition Parameter
Instrument : JCM-6000PLUS
Acc. Voltage : 15.0 kV
Probe Current: 1.00000 nA
PHA mode : T3
Real Time : 50.38 sec
Live Time : 50.00 sec
Dead Time : 0 %
Counting Rate: 1068 cps
Energy Range : 0 - 20 keV

Thin Film Standardless Standardless Quantitative Analysis
Fitting Coefficient : 0.1799

Element	(keV)	Mass%	Counts	Sigma	Atom%	Compound	Mass%	Cation	K
O K	0.525	26.57	5810.78	0.39	38.84				1.2308
Si K (Ref.)	1.739	73.43	19765.99	0.82	61.16				1.0000
Total		100.00			100.00				

View002

JEOL 1/1

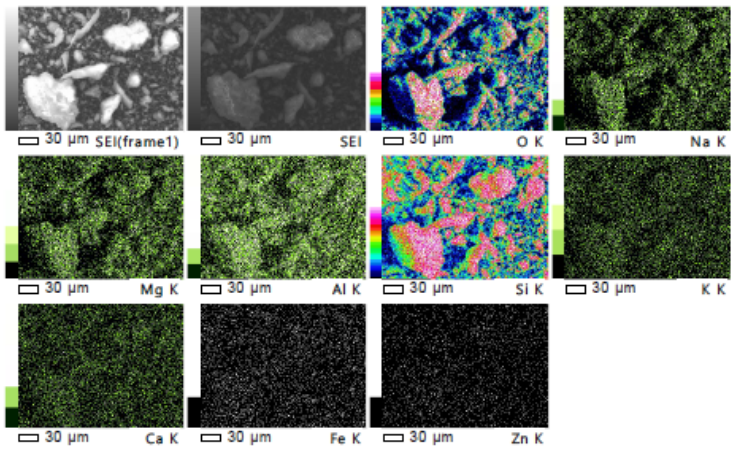


```
Date                : 4/1/2022
Resolution          : 256 x 192
--------------------------------
Instrument          : JCM-6000PL
Acc. Volt.          : 15 kV
Magnification       : x 500
Dwell Time          : 0.20 msec.
Sweep Count         : 50
```

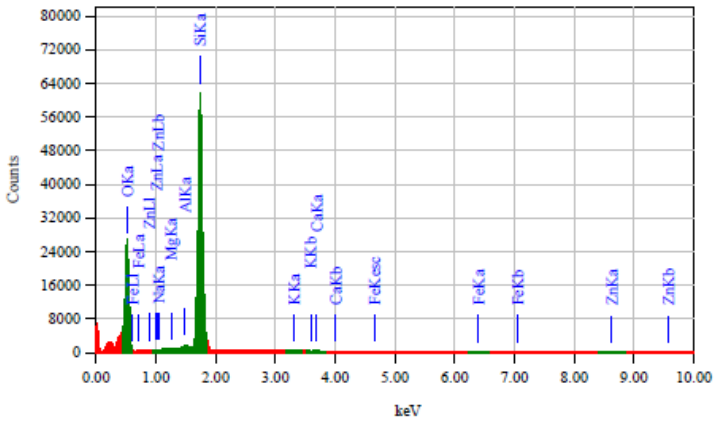


```
Acquisition Parameter
Instrument    : JCM-6000PLUS
Acc. Voltage  : 15.0 kV
Probe Current: 1.00000 nA
PHA mode      : T3
Real Time     : 491.52 sec
Live Time     : 485.81 sec
Dead Time     : 1 %
Counting Rate: 2401 cps
Energy Range  :  0 - 20 keV
```

View001

JEOL 1/1

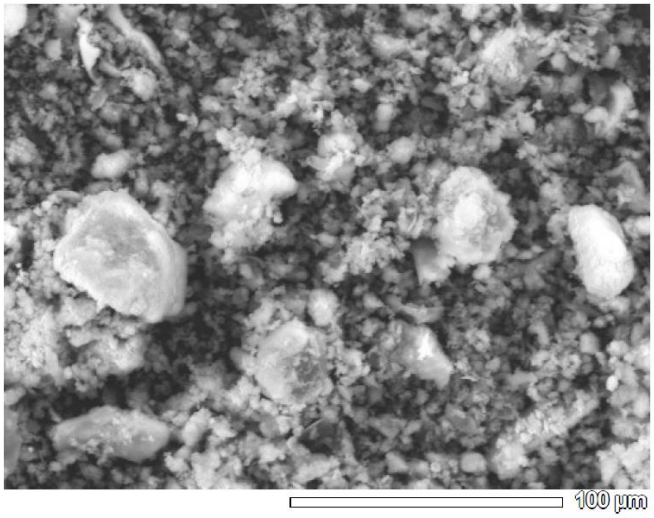

Title	: IMG1
Instrument	: JCM-6000PLUS
Volt	: 15.00 kV
Mag.	: x 500
Date	: 2022/04/01
Pixel	: 512 x 384

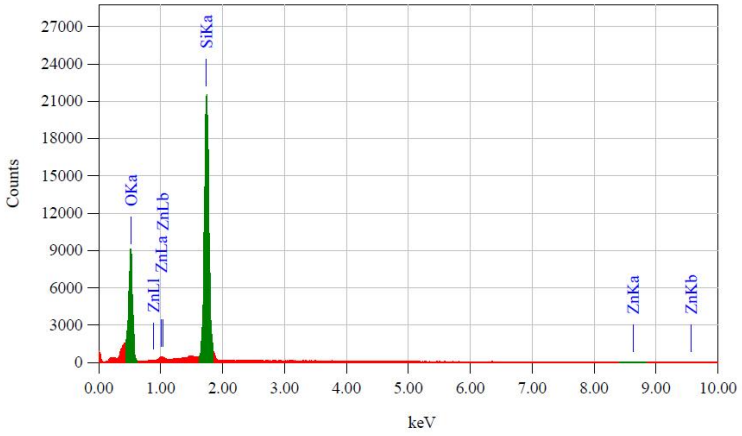

Acquisition Parameter
Instrument : JCM-6000PLUS
Acc. Voltage : 15.0 kV
Probe Current: 1.00000 nA
PHA mode : T3
Real Time : 51.16 sec
Live Time : 50.00 sec
Dead Time : 2 %
Counting Rate: 8032 cps
Energy Range : 0 - 20 keV

Thin Film Standardless Standardless Quantitative Analysis
Fitting Coefficient : 0.0833

Element	(keV)	Mass%	Counts	Sigma	Atom%	Compound	Mass%	Cation	K
O K	0.525	25.46	45901.08	0.13	37.71				1.2308
Si K (Ref.)	1.739	73.29	162622.47	0.28	61.84				1.0000
Zn K*	8.630	1.25	315.77	0.13	0.45				8.7519
Total		100.00			100.00				

View001

JEOL 1/1

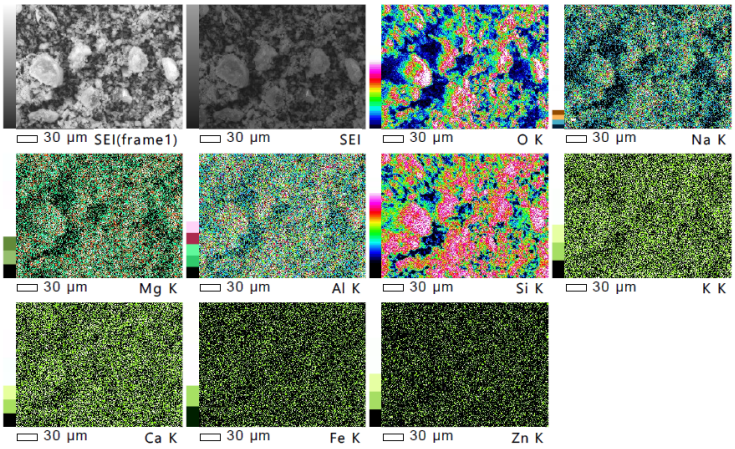

Date	: 4/1/2022
Resolution	: 256 x 192
Instrument	: JCM-6000PL
Acc. Volt.	: 15 kV
Magnification	: x 500
Dwell Time	: 0.20 msec.
Sweep Count	: 50

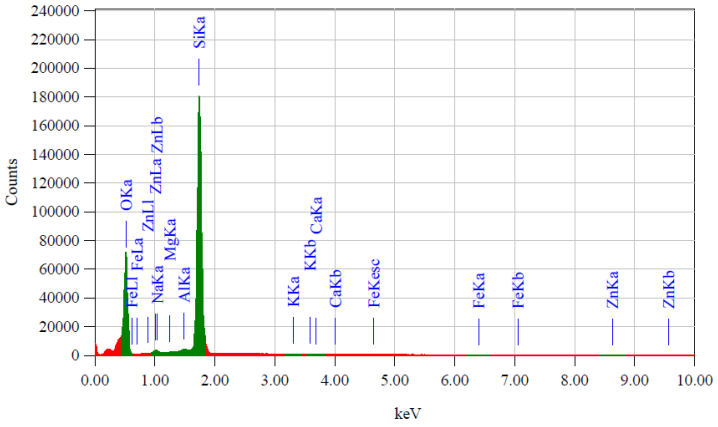

Acquisition Parameter

Instrument	: JCM-6000PLUS
Acc. Voltage	: 15.0 kV
Probe Current	: 1.00000 nA
PHA mode	: T3
Real Time	: 491.52 sec
Live Time	: 481.41 sec
Dead Time	: 2 %
Counting Rate	: 6810 cps
Energy Range	: 0 - 20 keV

Lampiran 19. Hasil BET-BJH

micromeritics

TriStar II 3020 2.00 TriStar II 3020 Version 2.00 Unit 1 Port 2 Serial #: 1108 Page 1

Sample: MCM-41 (K)
Operator: Serah
Submitter: 35392
File: C:\TriStar II 3020\data\SAMPEL\2022\Mei\Samp...\MCM-41 K.SMP

Started: 5/10/2022 12:53:55 PM
Completed: 5/10/2022 10:56:49 PM
Report Time: 5/12/2022 11:14:30 AM
Sample Mass: 0.3804 g
Cold Free Space: 32.5384 cm³
Low Pressure Dose: None
Automatic Degas: No

Analysis Adsorptive: N2
Analysis Bath Temp.: -195.850 °C
Thermal Correction: No
Warm Free Space: 11.1485 cm³ Measured
Equilibration Interval: 5 s
Sample Density: 1.000 g/cm³

Summary Report

Surface Area

Single point surface area at P/Po = 0.292620569:	907.2998 m²/g
BET Surface Area:	920.4266 m²/g
t-Plot Micropore Area:	36.4047 m²/g
t-Plot External Surface Area:	884.0218 m²/g
BJH Adsorption cumulative surface area of pores between 1.7000 nm and 300.0000 nm diameter:	1051.051 m²/g
BJH Desorption cumulative surface area of pores between 1.7000 nm and 300.0000 nm diameter:	1,093.4357 m²/g
D-H Adsorption cumulative surface area of pores between 1.7000 nm and 300.0000 nm diameter:	893.111 m²/g
D-H Desorption cumulative surface area of pores between 1.7000 nm and 300.0000 nm diameter:	1,078.6568 m²/g

Pore Volume

Single point adsorption total pore volume of pores less than 178.3964 nm diameter at P/Po = 0.989142729:	0.858957 cm³/g
t-Plot micropore volume:	0.016773 cm³/g
BJH Adsorption cumulative volume of pores between 1.7000 nm and 300.0000 nm diameter:	0.797760 cm³/g
BJH Desorption cumulative volume of pores between 1.7000 nm and 300.0000 nm diameter:	0.806738 cm³/g

Pore Size

Adsorption average pore width (4V/A by BET):	3.73286 nm
BJH Adsorption average pore diameter (4V/A):	3.0360 nm
BJH Desorption average pore diameter (4V/A):	2.9512 nm
D-H Adsorption average pore diameter (4V/A):	3.3896 nm
D-H Desorption average pore diameter (4V/A):	3.1012 nm

micromeritics

Sample: MCM-41 (K)
Operator: Sarah
Submitter: 35392
File: C:\TriStar II 3020\data\SAMPEL\2022\Mel\Samp...\MCM-41 K.SMP

Started: 5/10/2022 12:53:55 PM
Completed: 5/10/2022 10:56:49 PM
Report Time: 5/12/2022 11:14:30 AM
Sample Mass: 0.3804 g
Cold Free Space: 32.5384 cm³
Low Pressure Dose: None
Automatic Degas: No

Analysis Adsorptive: N2
Analysis Bath Temp.: -195.850 °C
Thermal Correction: No
Warm Free Space: 11.1485 cm³ Measured
Equilibration Interval: 5 s
Sample Density: 1.000 g/cm³

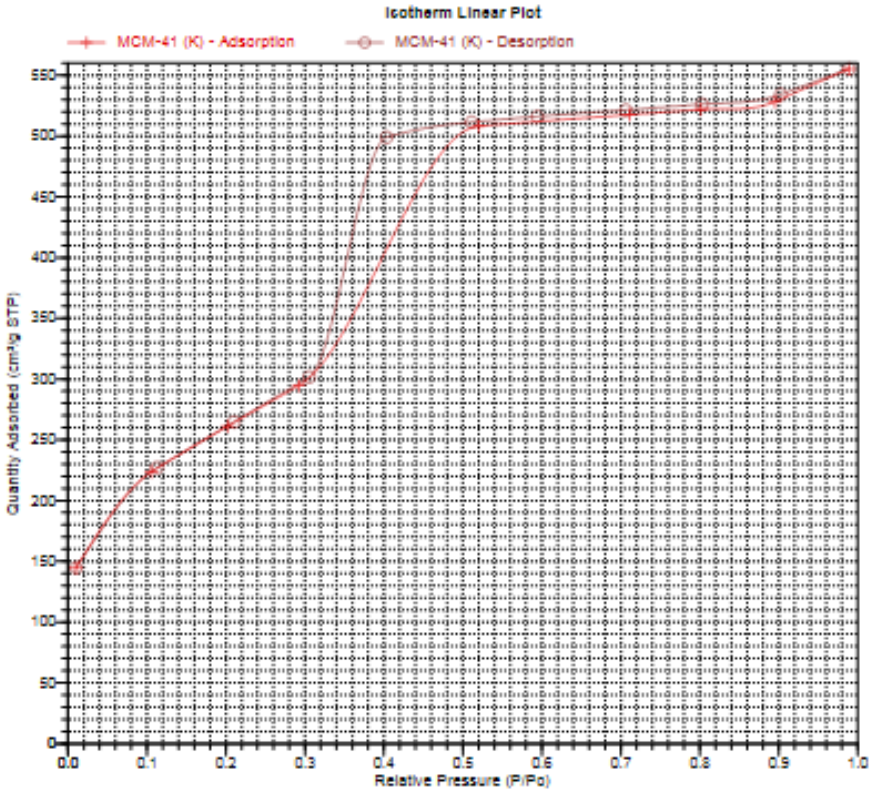

micromeritics®

Sample: Zn-MCM-41 (K)Zn
Operator: Sarah
Submitter: 35392
File: C:\TriStar II 3020\data\SAMPEL\2022\Me...\Zn-MCM-41-K-Zn.SMP

Started: 5/10/2022 12:53:55 PM
Completed: 5/10/2022 10:56:49 PM
Report Time: 5/12/2022 11:13:24 AM
Sample Mass: 0.3217 g
Cold Free Space: 32.9207 cm³
Low Pressure Dose: None
Automatic Degas: No

Analysis Adsorptive: N2
Analysis Bath Temp.: -195.850 °C
Thermal Correction: No
Warm Free Space: 11.2593 cm³ Measured
Equilibration Interval: 5 s
Sample Density: 1.000 g/cm³

Summary Report

Surface Area

Single point surface area at P/Po = 0.294254644:	883.3794 m²/g
BET Surface Area:	896.0407 m²/g
t-Plot Micropore Area:	28.7736 m²/g
t-Plot External Surface Area:	867.2671 m²/g
BJH Adsorption cumulative surface area of pores between 1.7000 nm and 300.0000 nm diameter:	1073.218 m²/g
BJH Desorption cumulative surface area of pores between 1.7000 nm and 300.0000 nm diameter:	1,066.5450 m²/g
D-H Adsorption cumulative surface area of pores between 1.7000 nm and 300.0000 nm diameter:	1027.269 m²/g
D-H Desorption cumulative surface area of pores between 1.7000 nm and 300.0000 nm diameter:	1,042.6978 m²/g

Pore Volume

Single point adsorption total pore volume of pores less than 173.0263 nm diameter at P/Po = 0.988800611:	0.833870 cm³/g
t-Plot micropore volume:	0.013062 cm³/g
BJH Adsorption cumulative volume of pores between 1.7000 nm and 300.0000 nm diameter:	0.787646 cm³/g
BJH Desorption cumulative volume of pores between 1.7000 nm and 300.0000 nm diameter:	0.784035 cm³/g

Pore Size

Adsorption average pore width (4V/A by BET):	3.72246 nm
BJH Adsorption average pore diameter (4V/A):	2.9356 nm
BJH Desorption average pore diameter (4V/A):	2.9405 nm
D-H Adsorption average pore diameter (4V/A):	3.1162 nm
D-H Desorption average pore diameter (4V/A):	3.0995 nm

micromeritics

Sample: Zn-MCM-41 (K)Zn
Operator: Sarah
Submitter: 35392
File: C:\TriStar II 3020\data\SAMPEL\2022\Me...\Zn-MCM-41-K-Zn.SMP

Started: 5/10/2022 12:53:55 PM
Completed: 5/10/2022 10:56:49 PM
Report Time: 5/12/2022 11:13:24 AM
Sample Mass: 0.3217 g
Cold Free Space: 32.9207 cm³
Low Pressure Dose: None
Automatic Degas: No

Analysis Adsorptive: N2
Analysis Bath Temp.: -195.850 °C
Thermal Correction: No
Warm Free Space: 11.2593 cm³ Measured
Equilibration Interval: 5 s
Sample Density: 1.000 g/cm³

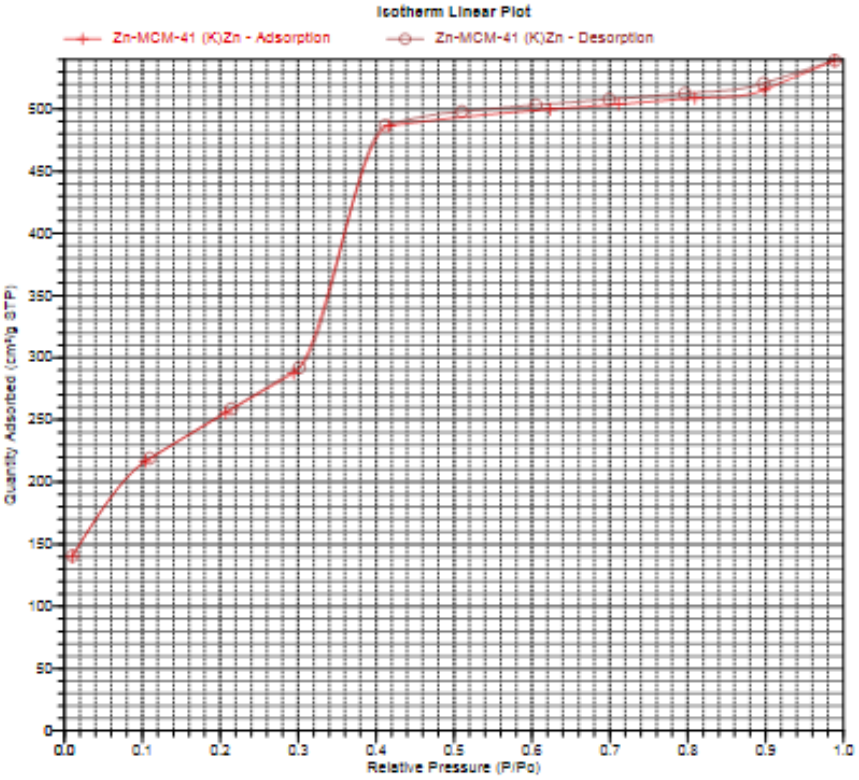

Lampiran 20. Dokumentasi Penelitian

1. Sintesis Material Zn-MCM-41

Pembuatan Natrium Silikat

Campuran gel
(Natrium silikat+Surfaktan)

Pemanasan

Penyaringan dan pencucian

Hasil Penyaringan

Serbuk MCM-41 dengan surfaktan

MCM-41 + Zink nitrat

Penyaringan dan pencucian

Serbuk Zn-MCM-41 dengan surfaktan

Kalsinasi

Zn-MCM-41

2. Studi Adsorpsi

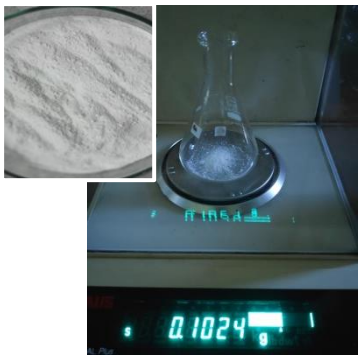

Serbuk Zn-MCM-41

Larutan Zat warna

Campuran adsorben+adsorbat di*shaker*

Penyaringan

Pengukuran absorbansi filtrat dengan spektronik 20D^{+}

Residu MK

Residu BCR